A multi-criteria approach to optimize the design-operation of Energy Communities considering economic-environmental objectives and demand side management

Enrico Dal Cin[a], Gianluca Carraro[a,]*, Gabriele Volpato[a], Andrea Lazzaretto[a], Piero Danieli[b]

[a] University of Padova, Industrial Engineering Department
Via Venezia 1, 35131 Padova, Italy
[b] University of Padova, Department of Management and Engineering
Stradella S. Nicola 3, 36100 Vicenza, Italy
enrico.dalcin@phd.unipd.it, gianluca.carraro@unipd.it, gabriele.volpato.1@phd.unipd.it, andrea.lazzaretto@unipd.it, piero.danieli@unipd.it
* corresponding author

Abstract

This paper focuses on three different configurations of energy communities (ECs) modelled as aggregations of local prosumers of renewable electric and thermal energy. The goal consists in improving the economic performance of the ECs while contributing to address the issue of climate change and fulfilling the existing energy demands or demands modified with smart strategies. Accordingly, type and size of the energy conversion and storage units of the prosumers included into ECs (design) and their operation are optimized with a bi-objective approach, considering investment and operation costs, and greenhouse gas emissions, both direct due to fuel burning, and indirect due to life cycle, as objectives to minimize. Moreover, two strategies of demand side management (DSM) are considered: a price-based demand response program applied downstream of the design optimization, and a new DSM model, which adapts the electricity demand to the renewable energy sources locally available, applied upstream of the design optimization. It results that the proposed DSM can ensure a better balancing between generation and demand profiles, thereby decreasing the stress on the electricity grid. Globally, ECs can reduce their energy expenditure of 14% and the overall CO_2-equivalent emissions of 24% compared to the reference case of the simple consumers.

Keywords

Energy Community, Multi-objective Optimization, Demand Side Management, Price-based Demand Response

1 Introduction

Global warming and climate changes require timely interventions, which must drastically reduce greenhouse gas (GHG) emissions to hit the target set by the Paris Agreement in 2015, i.e., to keep the global temperature rise well below 2°C at the end of the century [1]. By enacting legislative frameworks as the "Clean Energy for All Europeans" [2] and "Fit for 55" [3] packages, the European Union (EU) set the roadmap to reduce the GHG emissions of 55% by 2030 (compared to 1990 level) and achieve the carbon neutrality by 2050. Moreover, most of these directives concerns the energy sector, which is responsible for 75% of the global GHG emissions [4].

1.1 Object of the work

Within this framework, the Energy Communities could play an important role in fostering an economically, technically and environmentally sustainable transition [5]. An Energy Community (EC) is a group of private people, small and medium enterprises (SMEs) and local authorities that owns and operates a set of generation and storage systems and can consume, store or sell the energy produced. Despite several community energy projects already exist throughout Europe, only recently

the ECs have been legally defined by the EU legislation [6]. Precisely, the recast of the Renewable Energy Directive (RED II) of 2018 [7] introduced the Renewable Energy Community (REC), whereas the 2019 Internal Electricity Market Directive (IEMD) [8] defined the Citizen Energy Community (CEC). The REC can only exploit renewable energy sources (RES) to fulfil different kinds of demand (e.g., electrical and thermal), whereas the CEC can manage only electricity, both from RES and fossil fuels, and can operate in an autonomous microgrid.

The Italian government has only recently implemented the EU directives and framed the REC by means of a provision enacted by the national energy Authority (*ARERA*) [9]. However, differently from the European REC, the Italian REC can only manage electricity by RES and requires that its members be individually connected to the public distribution grid. The Energy Service Manager (the Italian *GSE*) provides an incentive rate of 11 c€/kWh for each kWh of community's Shared Electric Energy (SEE) [10], evaluated as the hourly minimum between the overall electricity fed into the grid by the REC and the overall electricity withdrawn from it. The Italian electricity market appears suitable for a wide diffusion of ECs. The residential sector accounts for 24% of the national electricity consumption, the industry for 40%, the tertiary sector for 30% and the agriculture for 2% [11]. By following the legislation, all users of the residential sector (private people) and SMEs are free to participate in EC projects. In Italy the share of SMEs among all the enterprises is higher than the average European value, accounting for 57% of the national production of goods and services [12]. Thus, a great share of customers of the Italian energy sector would have, by legislation, the possibility of joining EC projects. As a result, it is important to investigate the possible economic, environmental and energy benefits that ECs can bring to their members and to the entire energy system.

1.2 Literature review

ECs are covered quite extensively in the scientific literature. Several papers have dealt with their formation and modelling principles. Gjorgievski et al. [13] reviewed the design aspects (economic, environmental and social goals, involved technologies, design and optimization algorithms) and analysed impacts (economic, technical, environmental) of EC formation. They pointed out the usefulness of trade-off models between multiple objectives to get a more complete picture of possible impacts. The Mixed Integer Linear Programming (MILP) approach was recognized as the most used among design models due to its quickness, simplicity and adaptability to many problems (e.g., Rech [14] proposed a general MILP-based method to optimize the design and operation of distributed energy systems that can be also applied to ECs). Berka et al. [15] reviewed more in detail the local impacts deriving from ECs, such as raising awareness of environmental issues, development of knowledge and skills, and generation of socio-economic benefits for the community and community members. Differently, Hanke et al. [16] focused on social impacts and pointed out that a well-designed "enabling framework" could empower vulnerable consumers to participate in EC projects, providing them an active role in the energy transition.

Other papers evaluate the potential of EC in specific case studies [17-20]. Cheade and Dincer [21] modelled a poly-generational energy hub comprising a small modular nuclear reactor and a thermo-chemical loop for delivering thermal energy over long distances and fulfilling the thermal and electrical demand of a community. He et al. [22] proposed a hybrid peer-to-peer system for sharing electricity and hydrogen applied to a residential community in California and able to enhance the power supply reliability and grid stability, in response to intermittent renewable power generation. Vand et al. [23] designed an energy management system based on non-linear economic model predictive control and successive linear programming optimization for sharing the locally generated electricity between four buildings in a small community. The results shows that the annual electricity energy cost can be reduced of 7% on the community level compared to the buildings individually acting. Bracco et al. [24] optimized the design and operation of renewable and intermittent distributed generation in a district of Savona (Italy), with an economic objective based on a MILP algorithm. The analysed EC comprises some residential buildings and a school, and the considered RES are sun

and wind for electricity production, biomass for combined heat and power (CHP). Results showed that CHP units are economically effective only if the electrical and heating demands are comparable, and that generation plants must be chosen to guarantee a high self-consumption, rather than to sell electricity to the grid. Ruiz et al. [25] optimized the design-operation of a hybrid stand-alone power generation system in a rural community in Colombia by means of a MILP algorithm with an economic objective. The authors considered the presence of PV, Diesel internal combustion engines, batteries, electric vehicles and a microgrid that connects generators and users. They discovered that a high share of dispatchable sources is required (more than 60% of total generation comes from Diesel plants) to guarantee the cost-effectiveness of the project. Novoa et al. [26] modelled and optimized (by means of a single objective MILP algorithm) an EC including PV and batteries. By allocating optimally both generation and storage units in a real electricity grid of a city district, they obtained a zero net energy operation, a result that can be accomplished only by aggregating users in a community. Yan et al. [27] performed a Markovian-based stochastic optimization of the daily operation of distributed energy systems in a local EC, considering the intermittent and uncertain nature of renewable generation. Besides the economic objective of the optimization, they also considered a carbon tax to take into account the environmental impact.

It can be noted that, regardless of the case study considered and methods applied, none of the previous papers systematically compare different types of EC configurations.

Multi-objective optimization approaches are very useful for analysing a problem from various perspectives [13], although they have been rarely used in the study of ECs [28, 29]. Guo et al. [30] performed a very complete work for the multi-objective optimization of an energy community including different kinds of energy conversion units (PV, solar thermal, CHP internal combustion engines) and storage units (Lion batteries and thermal storage tanks). The goal is the search of the optimal generation share of each unit for assigned electric and thermal demands of the whole EC, with cost, external energy dependence and solar fraction as main objectives. Moreover, by means of Monte Carlo method and K-means clustering, they tried to predict the load on the source-side and load-side. Park et al. [31] dealt with the multi-objective optimization of the design of a RES-based generation system fulfilling the energy load of a residential apartment complex, with the aim of maximizing the RES generation while minimizing the investment costs. Fleischhacker at al. [32] considered the overall costs and emissions as competing objectives in a multi-objective function, by addressing only the operation of the analysed community. On the other hand, Liu et al. [33] applied the multi-objective optimization also to the design of an EC, still considering the EC only as a single entity with unique electrical, heating and cooling demands to be met. In all these works, the energy conversion and storage units serve the entire community, as if there were a district heating network, for the delivery of thermal energy to the users, besides the electric grid.

In recent years, an increasing number of studies focused on the consumption side of energy systems and several methods of demand side management (DSM) were and are being developed [34-36]. However, techniques of demand side management were applied to ECs only in few examples. An example of DSM is the demand response (DR), i.e., as defined by the U.S. Department of Energy, "*changes in electric usage by end-use customers from their normal consumption patterns in response to changes in the price of electricity over time, or to incentive payments designed to induce lower electricity use at times of high wholesale market prices or when system reliability is jeopardized*" [37]. Li et al. [38] introduced the DR into the electrical operation of an EC achieving a cost reduction of 3-5% in the energy expenditure, whereas Li and Yu [39] found out that a multi-energy DR program can benefit both the economic and environmental performance of the ECs. As last examples, Barreto et al. [40] and Zhou et al. [41] analysed how DR could be integrated with PV electricity generation. The first paper aimed at enhancing the management of the community's resources by means of DR, while the second one stated that DR can improve the PV profit of about 13%. However, in the above-mentioned works, the DR concerns only the operation of the ECs and is never integrated into or before the design phase.

Table 1 shows an overview of the EC-related case studies available in the literature focusing on the considered modelling aspects (also the proposed work is reported for comparison).

Table 1 *Comparison of the case studies found in the EC-related literature focusing on the considered modelling aspects.*

Reference	Operation optimization	Design optimization	Multi-objective optimization	DSM affecting the operation	DSM affecting the design	Aggregation of prosumers*
[24]	✓	✓				
[25]	✓	✓				
[26]	✓	✓				✓
[27]	✓					✓
[28]	✓	✓	✓			
[29]	✓	✓	✓			
[30]	✓	✓	✓			
[31]	✓	✓	✓			
[32]	✓		✓			
[33]	✓	✓	✓			
[38]	✓			✓		
[39]	✓			✓		✓
[40]				✓		
[41]	✓		✓	✓		
Proposed work	✓	✓	✓	✓	✓	✓

** The ECs are modelled as an aggregation of independent prosumers having their specific energy demands, and not as a unique entity with an overall demand given by the sum of the single ones.*

1.3 Novelty and goal

It emerges that the literature is still incomplete in:

- Comparing systematically different configurations of EC modelled as aggregations of prosumers with their own conversion/storage units and energy demands;
- Using multi-objective approaches to optimize the generation pattern of each prosumer belonging to the EC;
- Considering DSM programs as powerful tools that can improve the design of ECs with the aim of better exploiting the local RES.

This work contributes to fill in these research gaps by proposing a set of criteria to optimize the design and operation of different configurations of ECs that aggregate different prosumers of renewable energy with their own specific electrical and thermal loads (***Figure 1b***) and adhere to DSM programs. This approach widens the perspective of the more recent papers in the literature, which refer to energy conversion units that fulfil the entire needs of the EC (see ***Figure 1a*** and, e.g., [30]). In this latter case, the more or less implicit assumption is that the EC operates as if there were a single prosumer in it, and a single collector of the total thermal energy generated (like a district heating network).

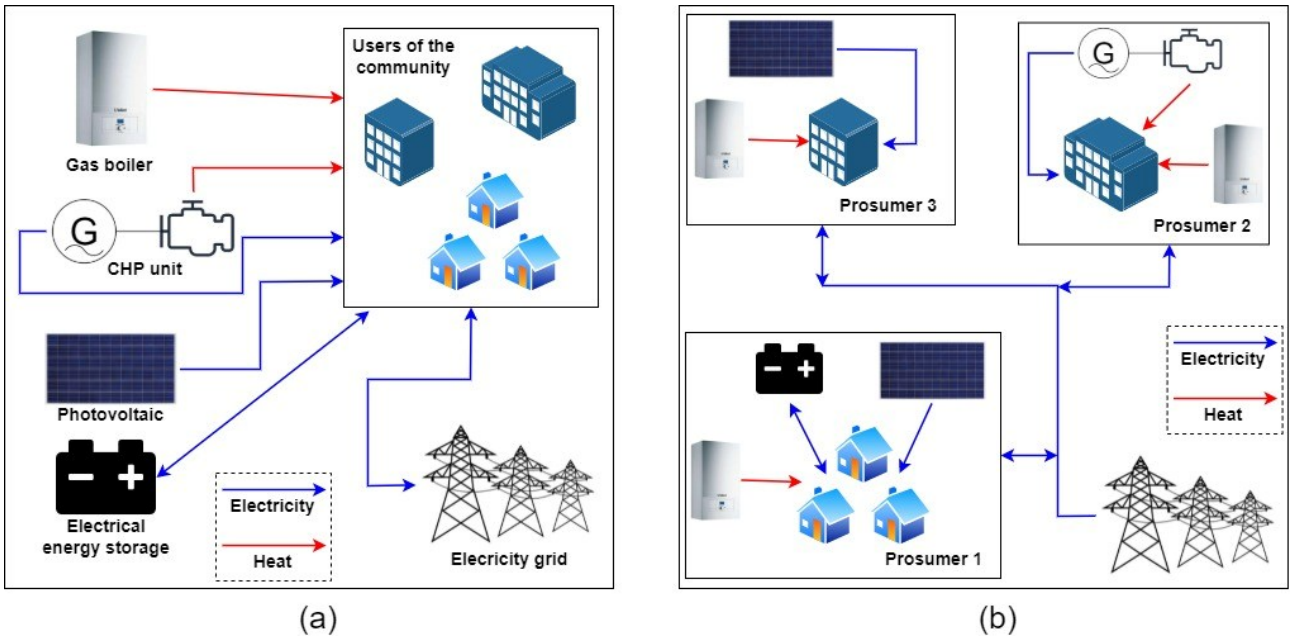

Figure 1 a) *EC with energy conversion and storage units supplying the total demands,* ***b)*** *EC as aggregation of prosumers with separate energy conversion and storage units, where the thermal energy generated satisfies the local demands.*

The goal is to determine the number, type and size of the conversion and storage units of each prosumer (design) and their operation in order to optimize the economic and environmental (GHG emissions) performances of the whole ECs compared to simple consumers and prosumers acting individually, while evaluating the level of self-consumption and the usage of the electricity grid.

The proposed criteria comprise:

1) A bi-objective optimization of the design-operation of ECs with an environmental objective (minimum GHG emissions, even considering life cycle parameters) and an economic objective (minimum overall cost);
2) A price-based demand response (PBDR) program that optimizes the electrical demand downstream of 1) and aims at minimizing the expenditures for electricity purchase;
3) Alternatively to 2), a DSM program applied upstream of 1) which aims at adapting the profile of electrical demand to the available RES with the purpose of increasing the generation by RES and its local self-consumption.

The novelty of the proposed DSM applied upstream of the design phase is that it affects the selection of the optimal number, type and size (design) of the conversion and storage units fulfilling the improved demands. Thus, differently from a traditional DR approach concerning only the operation of an EC, this strategy allows better fitting the generation pattern to the pursued objectives.

A specific case study is analysed to show the potentialities of the proposed criteria. This case study considers a small community (comprising two commercial users and a cluster of residential ones, with their electrical and thermal loads) hypothetically located in Padua (north-east of Italy). By following the European and Italian legislation, three different types of prosumers aggregation into an EC are modelled and optimized. The optimization is based on a Mixed Integer Programming (MIP) approach solved by means of the Gurobi software [42] in Python environment. In particular, the first criterion (bi-objective optimization) relies on a Mixed Integer Quadratic Programming (MIQP) algorithm. In spite of the higher computational time with respect to a MILP algorithm of the same size (i.e., the same number of decision variables), a MIQP approach is more accurate in describing complex systems with constraints that cannot be easily represented as linear [43].

2 Methods

2.1 Modelling of the Energy Communities

A representative case study is analysed to show the potentialities of the proposed methods. As stated in *Section 1.1* the Italian electricity market appears to be suited for a large diffusion of ECs, especially considering the residential and tertiary sectors that together account for 54% of the overall national electricity consumption [11]. Therefore, this paper deals with a hybrid residential-commercial cluster of users, which includes two commercial utilities and a residential one. Each of them can be equipped with the most suitable generation and storage units in the context of distributed generation such as photovoltaic (PV) plants, thermal solar collectors (TSC), combined heat and power (CHP) plants.

2.1.1 Input data

All the time-variable input data are compressed into four typical days, one representative for each season of the year, so that the reference yearly period is composed of 96 hourly values (h). The winter day is defined in the range of hours from h = 1 to h = 24, spring from 25 to 48, summer from 49 to 72, and autumn from 73 to 96.

Three different types of users are analysed, and they are supposed to be located in Padua in the north-east of Italy (latitude = 45° North, longitude = 11° East). Two of these users are commercial users (a restaurant, referred to as *Com1*, and an office building, *Com2*) while the third is a cluster of 14 residential buildings (referred to as *Res*). The electrical (D_{el}) and heating (D_{th}) demands [44] are reported in ***Figure 2*** and ***Figure 3***, respectively, for each user and their aggregation (*Agg*, sum of the single demands).

The required meteorological data, imported from the database of the European Photovoltaic Geographical Information System (PVGIS) [45] for Padua, are the ambient temperature and the solar irradiance on the horizontal plane. They are reported in ***Figure 4*** for each typical day.

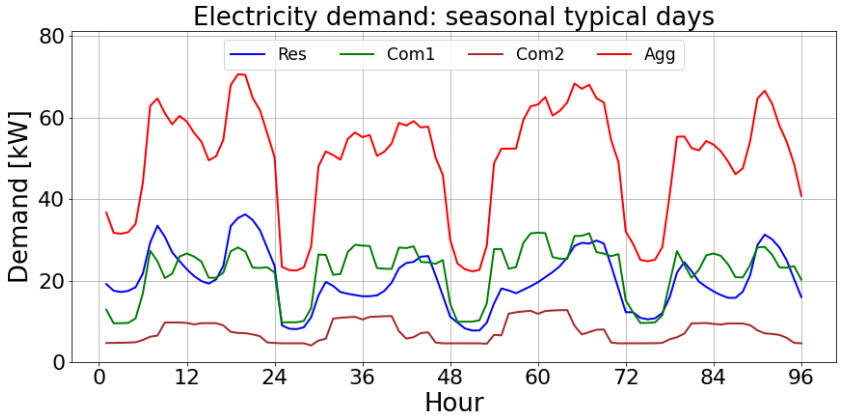

Figure 2 *Residential (blue), commercial (green and brown) and aggregated (red) electricity demand for the seasonal typical days.*

The electricity selling price (p_e) corresponds to the wholesale electricity market price and is taken from the Italian Energy Market Manager (*GME*) database [46], while the purchasing cost (c_e) follows the same trend but is higher because of the transmission and distribution costs and other fees [47]. These costs are reported in ***Figure 5*** for the considered reference period. The natural gas cost for the final user (c_g) is assumed to be constant and equal to 1 €/m^3 [47]. Also, the biogas cost (c_{bg}) is constant and corresponds to its production cost equal to 7.5 c€/kWh (referred to the biogas energy content considering the low heating value) [48].

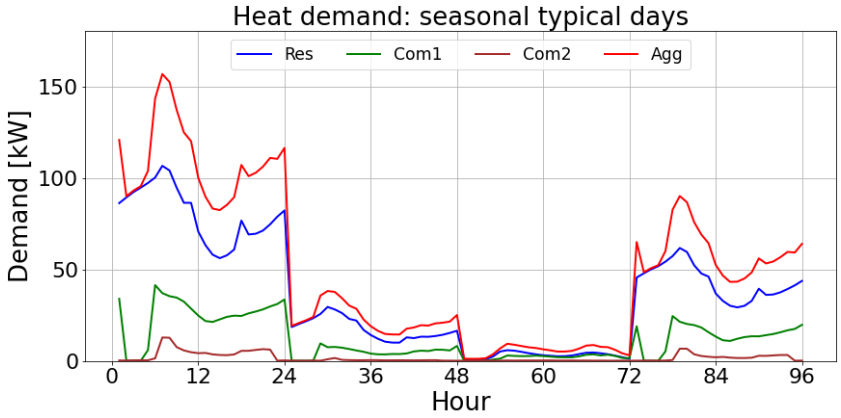

Figure 3 *Residential (blue), commercial (green and brown) and aggregated (red) heat demand for the seasonal typical days.*

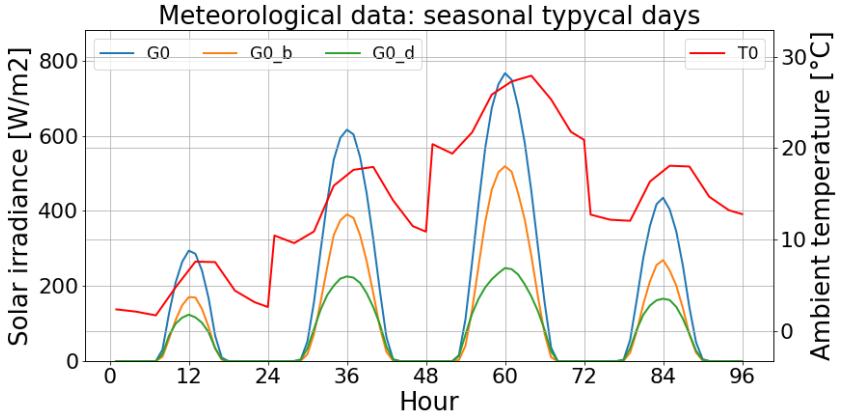

Figure 4 *Global (blue), beam (orange) and diffuse (green) solar irradiance on the horizontal plane, and ambient temperature (red) for the seasonal typical days.*

Figure 5 *Electricity selling price (purple) and purchasing cost (green) comparison for the seasonal typical days.*

2.1.2 Generation and storage units

The conversion units are photovoltaic panels (PV), thermal solar collectors (TSCs), combined heat and power (CHP) plants (internal combustion engines, ICEs) while the storage units are thermocline tanks and lithium batteries.

The electric power generated by a PV system (P_{PV}) is:

$$P_{PV} = G_{\beta} \cdot \eta_{el,PV} \cdot n_{PV} \cdot A_{PV}, \quad (1)$$

where n_{PV} is the number of installed PV panels, A_{PV} the specific area of one PV panel (1 m^2), $\eta_{el,PV}$ the net electrical efficiency (12.8 % by considering a nominal inverter efficiency of 95 % [49]) and

G_β is the global irradiance on a tilted surface (30 ° to the South [50]), calculated by following the Liu and Jordan model [51] and by assuming that the diffuse radiation is only isotropic [52].

The heat flow (thermal power) generated by a number n_{TSC} of thermal solar collectors is:

$$Q_{TSC} = G_\beta \frac{A_{op}}{A_{TSC}} \eta_{th,TSC} \cdot n_{TSC} \cdot A_{TSC},$$

(2)

where A_{op} is the opening area, A_{TSC} the total area of one solar panel and $\eta_{th,TSC}$ the thermal efficiency, calculated according to the *UNI EN ISO 9806* standard.

It is assumed that all the CHP units are fuelled by biogas, which is considered a renewable source by the European legislation [7]. However, in this work, biogas is not considered as a purely RES in order to assess the GHG emissions associated with its combustion. The technical data of the CHP units, four different sizes of ICE (*ice1*, *ice2*, *ice3* and *ice 4*), are reported in ***Table 1*** [53]. It is assumed that the electrical efficiency (η_{el}) of the CHP units decreases linearly from the nominal power (P_n) to the minimum deliverable power (P_{min}), and that under P_{min} these units are switched off because they would work in an inefficient way. Therefore, the electric power delivered by a CHP unit is:

$$P_i = \eta_{el,i} \cdot F_i - \sigma_i(\eta_{th,i} \cdot F_i - Q_i), for\ i \in \{ice1, ice2, ice3, ice4\}\ and\ P_{min,i} \leq P_i \leq P_{nom,i},$$

(3)

where Q is the delivered thermal power, that is:

$$Q_i \leq \eta_{th,i} \cdot F_i, for\ i \in \{ice1, ice2, ice3, ice4\}.$$

(4)

F is the power content of the input stream of fuel (biogas), η_{th} is the thermal efficiency (constant), and σ is a penalization coefficient that takes into account the power subtracted by the auxiliary components to dispose of the heat generated but not delivered to users ($\eta_{th,i} \cdot F_i - Q_i$). Thus, σ approximately considers the electric power required by the cooling system.

Table 1 *Technical data of the biogas-fuelled CHP units [53].*

		ice1	*ice2*	*ice3*	*ice4*
Nominal power	P_n [kW]	15	30	45	60
Minimum deliverable power	P_{min} [kW]	7.5	15	22.5	30
Electrical efficiency at nominal power	$\eta_{el}(P_n)$ [%]	30	32	34	36
Electrical efficiency at minimum power	$\eta_{el}(P_{min})$ [%]	26	28	30	32
Thermal efficiency	η_{th} [%]	55	55	55	55
Penalization coefficient	σ [%]	2	2	2	2

It is assumed that each user already owns a gas boiler (GB) with a constant thermal efficiency ($\eta_{th,gb}$) equal to 90%. The generated thermal power (Q_{gb}), as a function of the power content of the input fuel (F_{gb}), is:

$$Q_{gb} = \eta_{th,gb} \cdot F_{gb}.$$

(5)

The considered thermal energy storage (TES) is based on thermocline tanks in which water stratifies. From a modelling point of view hot and cold water are considered as sharply separated, thereby the system charge consisting in an increase of the hot water volume (V_{hot}). The round-trip efficiency of the TES (η_{tes}), equal to 98 %, is assumed as equally distributed between charging and discharging phases [48]. If V_{hot} is known at the time t, the hot water volume after a time interval Δt is calculated as:

$$V_{hot}(t+\Delta t) = V_{hot}(t) + \int_{t}^{t+\Delta t} \left(\frac{Q_{c,tes}}{\rho_w \cdot cp_w \cdot (T_{hot} - T_{cold})} \sqrt{\eta_{tes}} - \frac{Q_{d,tes}}{\rho_w \cdot cp_w \cdot (T_{hot} - T_{cold})} \frac{1}{\sqrt{\eta_{tes}}} \right) dt, \quad (6)$$

where ρ_w is the water density (1000 kg/m^3), cp_w the specific heat (4.18 kJ/kg/K), Q_c the charging thermal power provided in input to the storage, Q_d the discharging thermal power required in output, T_{hot} (80°C) and T_{cold} (50°C) the hot- and cold-side temperatures of the water in the tank, respectively. The upper bound of the hot water volume is given by the size of the storage tank (V_{tes}) while the lower bound is zero (completely discharged TES, all volume filled by cold water):

$$0 \leq V_{hot} \leq V_{tes}. \quad (7)$$

The electric energy storage (EES) is given by lithium-based batteries. The round trip efficiency of the EES (η_{ees}), equal to 87% [48], is assumed to be uniformly distributed between charging and discharging phases. A full charge means a State of Charge (SoC) equal to 100 %. However, to do not deteriorate cells, the minimum SoC cannot be lower than the 50% of the battery capacity (C_{ees}) [54]. By knowing the SoC of the battery, i.e., the contained energy (E_{ees}), at the time t, E_{ees} after a time interval Δt is calculated as follows (self-discharge is neglected):

$$E_{ees}(t+\Delta t) = E_{ees}(t) + \int_{t}^{t+\Delta t} \left(P_{c,ees} \sqrt{\eta_{ees}} - \frac{P_{d,ees}}{\sqrt{\eta_{ees}}} \right) dt, \quad (8)$$

where P_c and P_d refer to the charging electric power provided in input to the battery and the discharging electric power required in output, respectively. The constraints on E_{ees} are:

$$0.5 C_{ees} \leq E_{ees} \leq C_{ees}. \quad (9)$$

The assumed specific investment cost and operation and maintenance (*O&M*) costs (fixed and variable: $c_{O\&M,fix}$ and $c_{O\&M,fix}$, respectively) are reported in ***Table 2*** for each technology [53, 55-57]. The investment costs are subsequently actualized (and referred to as C_a) by considering 20 years of expected lifetime and a discount rate of 3 % [58]. Since it is assumed that each user owns a gas boiler by default, the GB investment cost is not considered.

Table 2 *Specific investment and O&M costs of the considered conversion and storage units [53, 55-57].*

Generation and storage units	Specific investment cost	Fixed O&M cost	Variable O&M cost
PV	250 €/panel	12.5 €/m^2/year	-
TSC	860 €/panel	8.5 €/panel/year	-
ice1	3000 €/kW	100 €/kW/year	0.6 c€/kWh$_{fuel}$
ice2	2800 €/kW	100 €/kW/year	0.6 c€/kWh$_{fuel}$
ice3	2600 €/kW	100 €/kW/year	0.6 c€/kWh$_{fuel}$
ice4	2400 €/kW	100 €/kW/year	0.6 c€/kWh$_{fuel}$
GB	-	-	0.5 c€/kWh$_{fuel}$
TES	175 €/m^3	8.75 €/m^3/year	-
EES	1500 €/kWh	8 €/kWh/year	-

2.1.3 Emission factors

A specific emission factor (*ef*) is assigned to each conversion or storage unit to assess its GHG emissions. Each emission factor is obtained by the sum of direct emissions, caused by fuel combustion, and indirect equivalent emissions, produced during the life cycle of the specific technology. Hence, also the environmental impact of RES-based technologies is evaluated. The specific life-cycle contributions are taken from studies on the Life Cycle Analysis available in the scientific literature [59-62]. A constant emission factor is also associated with the electricity

withdrawn from the grid (ef_{gw}) and depends on the generation mix that feeds the grid itself [63]. All the considered emission factors are reported in ***Table 3***.

Table 3 *Contributions to GHG emissions and emission factors [59-63].*

Technology	Direct contribution	Indirect (LCA) contribution	Emission factor (*ef*)
Electricity grid	-	-	0.356 kg/kWh$_{el}$
PV	-	0.066 kg/kWh$_{el}$	0.066 kg/kWh$_{el}$
TSC	-	0.024 kg/kWh$_{th}$	0.024 kg/kWh$_{th}$
ice1	0.197 kg/kWh$_{fuel}$	0.020 kg/kWh$_{fuel}$	0.217 kg/kWh$_{fuel}$
ice2	0.197 kg/kWh$_{fuel}$	0.020 kg/kWh$_{fuel}$	0.217 kg/kWh$_{fuel}$
ice3	0.197 kg/kWh$_{fuel}$	0.020 kg/kWh$_{fuel}$	0.217 kg/kWh$_{fuel}$
ice4	0.197 kg/kWh$_{fuel}$	0.020 kg/kWh$_{fuel}$	0.217 kg/kWh$_{fuel}$
GB	0.197 kg/kWh$_{fuel}$	negligible	0.197 kg/kWh$_{fuel}$
TES	-	100 kg/m^3$_{volume}$	100 kg/m^3$_{volume}$
EES	-	72.9 kg/kWh$_{capacity}$	72.9 kg/kWh$_{capacity}$

2.1.4 Organizations of prosumers

The simplest way that the users have to meet their electrical and thermal demands is to withdraw the electricity from the grid and to exploit their gas boilers, respectively. In such a way, the users act passively as simple consumers (i.e., no energy is locally generated or stored). Passive users are taken as the reference case (REF).

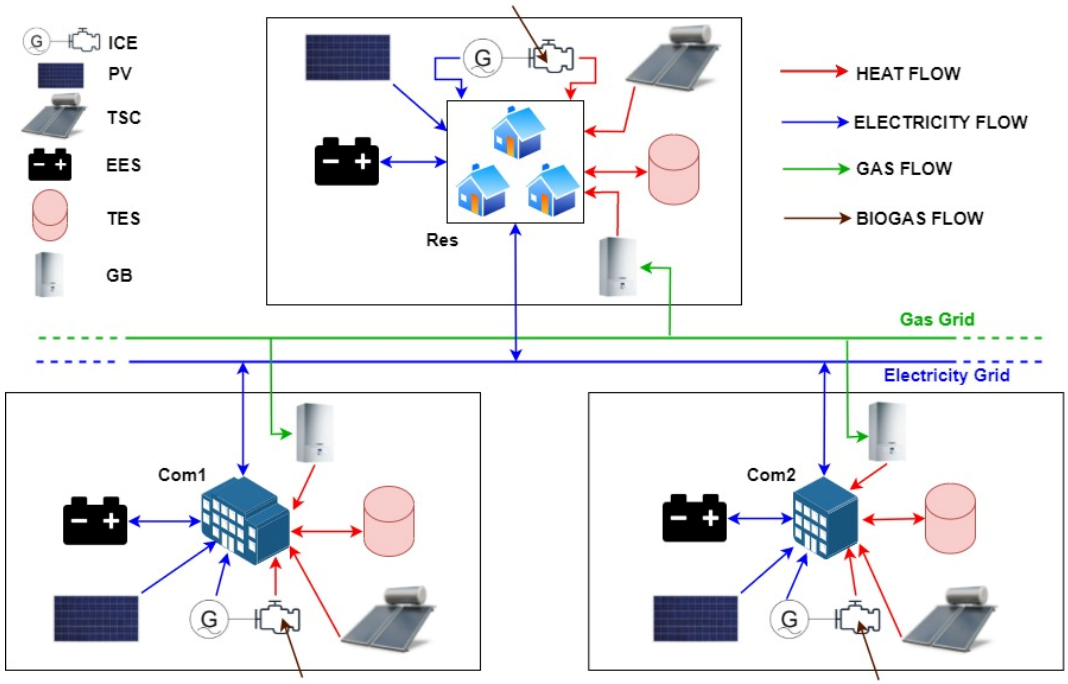

Figure 6 *Individual Prosumers (IP) configuration: representation of the possible plants and energy flows.*

In the first considered configuration, the prosumers are located on the distribution grid and operate individually without interacting among them (Individual Prosumers, IP). ***Figure 6*** reports a representation of the IP configuration, which is different from a configuration of energy community (e.g., citizen and renewable energy communities described hereinafter). The electric energy balance is defined as follows for each user:

$$D_{el,j,h} = P_{gw,j,h} - P_{gf,j,h} + P_{PV,j,h} + \sum_i P_{i,j,h} + P_{d,ees,j,h} - P_{c,ees,j,h},\ for\ j \in \{Res, Com1, Com2\}, i \in \{ice1, ice2, ice3, ice4\}\ and\ h \in [1,96], \quad (10)$$

where D_{el} is the electrical demand, P_{gw} is the electric power withdrawn from the grid, P_{gf} is the electric power fed into the grid, P_{PV} is the electric power generated by PV, calculated from *Eq.(1)*,

P_i is the electric power generated by the CHP units, calculated from *Eq. (3)*, $P_{d,ees}$ and $P_{c,ees}$ are the discharging and charging power of the EES, respectively. Each user individually and physically self-consumes a share of the electricity generated by itself and exchanges with the grid eventual surpluses or defects of production.

The heat balance for each user is:

$$D_{th,j,h} = Q_{gb,j,h} + Q_{TSC,j,h} + \sum_i Q_{i,j,h} + Q_{d,tes,j,h} - Q_{c,tes,j,h},$$
$$for\ j \in \{Res, Com1, Com2\}, i \in \{ice1, ice2, ice3, ice4\}\ and\ h \in [1,96], \quad (11)$$

where D_{th} is the thermal demand, Q_{gb} is the thermal power generated by gas boilers, Q_{TSC} is the thermal power generated by TSC, calculated from *Eq.(2)*, Q_i is the heat provided by the CHP units, *Eq.(4)*, $Q_{d,tes}$ and $Q_{c,tes}$ are the discharging and charging heat of the TES, respectively.

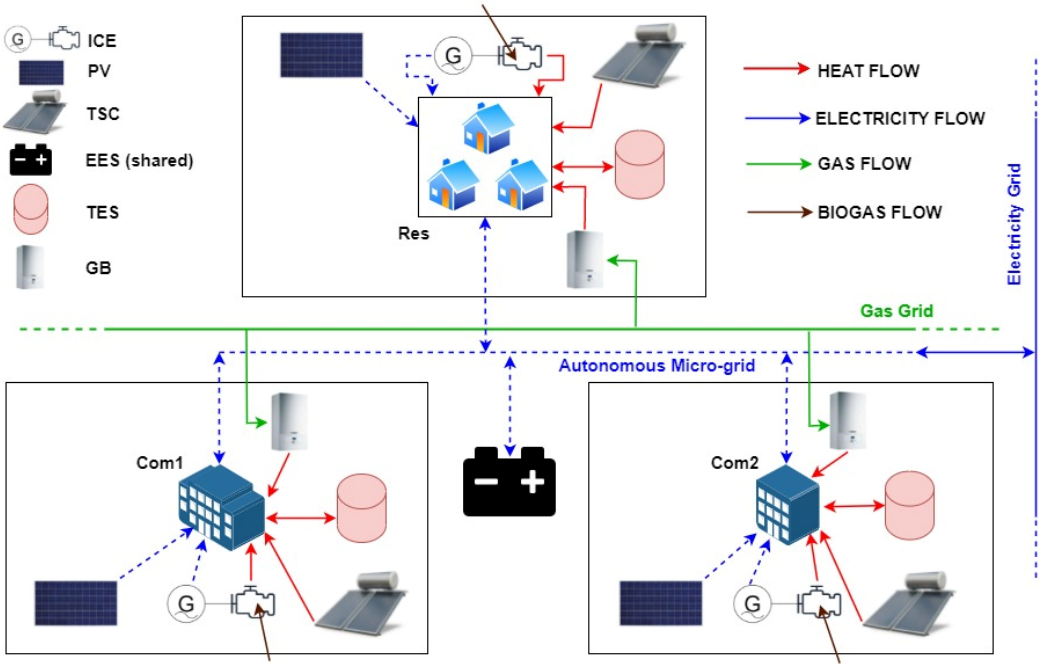

Figure 7 *Citizen Energy Community (CEC) configuration: representation of the possible plants and energy flows. Dashed flows are only hypothetical, they are not individually evaluated by the model.*

The first configuration of EC to be considered is the Citizen EC (CEC), as defined by the IEMD. The CEC itself and CEC members can own both RES-based and conventional electricity power plants (however, in this paper only RES are considered as primary sources for electricity generation in order to have a comparison with the other EC configurations under the same conditions) and can operate in an autonomous microgrid. Thus, it is assumed that the electricity generated by the prosumers is shared within the autonomous microgrid, hypothetically granted in concession to the CEC as an incentive. The latter is connected, in turn, to the public distribution grid through a single connection point. ***Figure 7*** shows a CEC configuration, which collectively and physically self-consumes a share of the electricity generated by all its members (eventually, even by means of a shared EES) and exchanges possible surpluses and defects with the public grid. The electric energy balance is defined for the entire CEC:

$$\sum_j D_{el,j,h} = P_{gw,h} - P_{gf,h} + \sum_j \left(P_{PV,j,h} + \sum_i P_{i,j,h} \right) + P_{d,ees,h} - P_{c,ees,h}, for\ j$$
$$\in \{Res, Com1, Com2\}, i \in \{ice1, ice2, ice3, ice4\}\ and\ h \in [1,96].$$
$$(12)$$

It is assumed that users are not close enough to make a district heating network cost effective. Thus, users must autonomously fulfil their thermal demand. Hence, the heat balance is specific for each user and analogous to *Eq. (11)*.

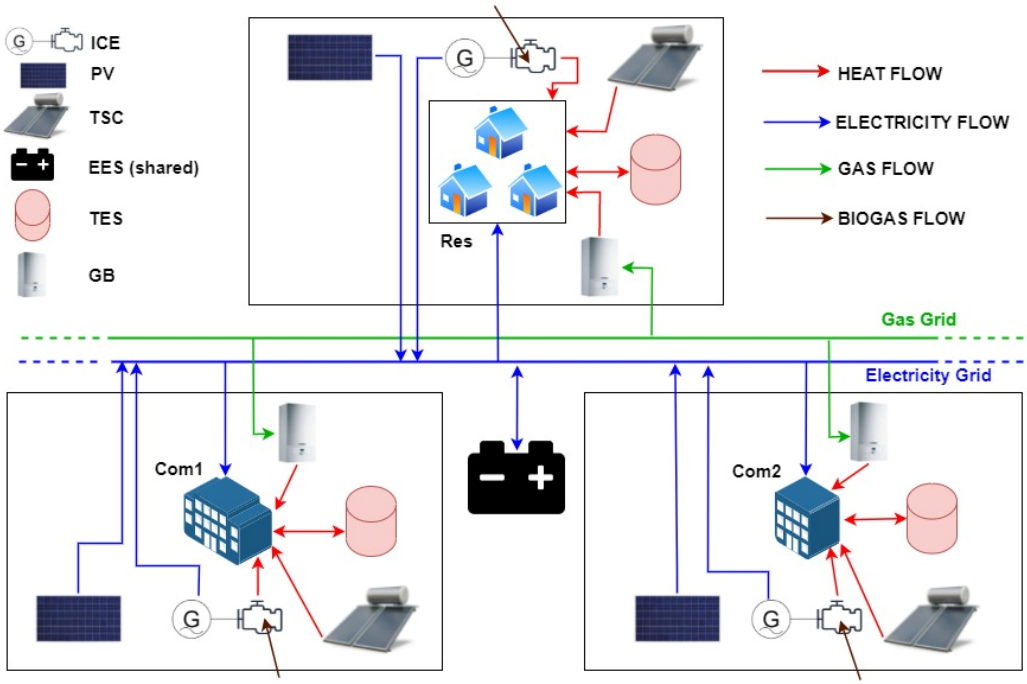

Figure 8 *Renewable Energy Community (REC) configuration: representation of the possible plants and energy flows.*

Another possible EC configuration is the Renewable EC (REC), as defined by the Italian legislation. The REC and its member can only own RES-based conversion unit and, furthermore, the REC members must be directly connected to the public electrical distribution grid. ***Figure 8*** shows a representation of the REC configuration, where also a shared EES is available. The whole amount of electricity generated and required by the prosumers has to be injected to and withdrawn from the grid, respectively. Moreover, the Shared Electric Energy (SEE), as defined by the Italian legislation, is hourly calculated and receives an incentive tariff (p_{sh} = 11 c€/kWh) [10]. Thus, the collective self-consumption is not physical but virtual, because the SEE is not directly exchanged among users but flows through the distribution grid. However, from a wider point of view, the energy flows associated with the SEE remain bounded within the section of the distribution grid where the REC is placed.

The electric energy balance is unique for the entire REC and composed of two equations:

$$\sum_j P_{gw,j,h} = P_{c,ees,h} + \sum_j D_{el,j,h}, for\ j \in \{Res, Com1, Com2\}\ and\ h \in [1,96], \quad (13)$$

and

$$\sum_j P_{gf,j,h} = P_{d,ees,h} + \sum_j \left(P_{PV,j,h} + \sum_i P_{i,j,h} \right), for\ j \in \{Res, Com1, Com2\}, i \in \{ice1, ice2, ice3, ice4\}\ and\ h \in [1,96]. \quad (14)$$

The SEE (E_{sh}) is calculated for the entire community in each hour as follows:

$$E_{sh,h} = min\left\{\sum_j P_{gw,j,h}\,;\sum_j P_{gf,j,h}\right\}, for\ j \in \{Res, Com1, Com2\}\ and\ h \in [0{,}96].$$

(15)

Also in this case, it is assumed that there is not any district heating network available. Thus, the heat balance is the same of *Eq. (11)*.

In this paper, the Hybrid Community (HC) is proposed as a new configuration containing elements of both IP and REC. The HC meets the requirements of the RED II (European REC) but not of the Italian legislation (which requires that the RES-based conversion units inject the entire amount of generated electricity into the grid) and, so, differs from the REC considered here. In fact, the HC has the same structure shown in ***Figure 6***, accordingly to the IP configuration. However, differently from IP, the surpluses and defects of electric generation exchanged with the grid are included in the calculation of the SEE, similarly to the REC. Thus, the self-consumption is partially individual and physical (as for the IP) and partially collective and virtual (as for the REC). The advantage of this configuration is that it is simpler than the CEC because it does not require an autonomous microgrid, whereas all users are directly connected to the public distribution grid. Moreover, differently from the REC, each user can physically self-consume part of the energy generated by itself, therefore maintaining a higher degree of independence.

Both the electric and thermal energy balances are the same of *Eqs. (10)* and *(11)*, while the SEE, which receives the incentive tariff p_{sh}, is calculated as in *Eq. (15)*.

2.2 Design and operation optimization

The design and operation optimization of the considered configurations of prosumers is carried out by means of a bi-objective MIQP algorithm. The two analysed objective functions, which describe the overall GHG emissions (f_1) and overall costs (f_2), are linearly combined into a global one (*f*) by two complementary weights, w_1 and w_2, applied to f_1 and f_2, respectively:

$$f = w_1 \cdot f_1 + w_2 \cdot f_2, with\ w_1 = 1 - w_2\colon\ w_1 \in [0{,}1], w_2 \in [0{,}1].$$

(16)

The plot of the two specific objectives, f_1 and f_2, as the weights vary, is the so called "Pareto front", and the obtained set of solutions is called "Pareto optimal" (i.e., no other feasible solutions have a performance at least equal in all the objectives, but strictly better in at least one of them [64]). To maintain the computational time acceptable, w_1 varies iteratively from 1 to 0 with uniform 0.1 intervals. Thus, the optimization is repeated 11 times for each configuration of prosumers.

2.2.1 Decision variables

The task of the optimization is to find out the set of values of the decision variables that minimizes the global objective function f. ***Table 4*** reports the arrays of the decision variables with their size for each configuration of prosumers. n_{PV} and n_{sol} are integer variables defined in the range [0;+∞), whereas δ_i are binary variables that can only assume 0-1 values, which describe the inclusion (δ_i = 1) or exclusion (δ_i = 0) of the *i-th* CHP unit into or from the design of a certain configuration. All the other variables are continuous and defined in the range [0;+∞).

2.2.2 Objective function

The two objectives are the overall GHG emissions (f_1) and the overall cost (f_2). For the IP and HC configurations, f_1 is described by the following equation:

$$f_1 = \sum_j \Bigg[C_{ees,j} \cdot ef_{ees} + V_{tes,j} \cdot ef_{tes} + \sum_{h=1}^{96} \Bigg(P_{gw,j,h} \cdot ef_{gw} + F_{gb,j,h} \cdot ef_{gb} + P_{PV,j,h} \cdot ef_{PV} + Q_{TSC,j,h} \cdot ef_{TSC} + \sum_i \delta_{i,j} \cdot F_{i,j,h} \cdot ef_i \Bigg) \Bigg] - \sum_{h=1}^{96} E_{sh,h} \cdot ef_{gw} \, , for \; j \in \{Res, Com1, Com2\} \; and \; i \in \{ice1, ice2, ice3, ice4\},$$

(17)

where E_{sh} is only defined for HC, and, since it represents the virtually self-consumed renewable energy, it is associated with a reduction of the GHG emissions caused by the withdrawal from the grid.

Table 4 *Arrays of decision variables with their size for the different configurations of prosumers. n_u refers to the number of utilities (= 3), n_m to the number of CHP units (= 4) and n_h to the number of hours in the reference period (= 96).*

Arrays of the decision variables		**Size of the arrays for each configuration**			
		IP	**CEC**	**REC**	**HC**
P_{gw}	Electric power withdrawn from the grid	n_u x n_h	n_h	n_h	n_u x n_h
P_{gf}	Electric power fed to the grid	n_u x n_h	n_h	n_h	n_u x n_h
P_i	Electric power generated by CHP units	n_m x n_u x n_h	n_m x n_u x n_h	n_m x n_u x n_h	n_m x n_u x n_h
$\eta_{el,i}$	Electrical efficiency of CHP units	n_m x n_u x n_h	n_m x n_u x n_h	n_m x n_u x n_h	n_m x n_u x n_h
F_i	Power content of input fuel of CHP units	n_m x n_u x n_h	n_m x n_u x n_h	n_m x n_u x n_h	n_m x n_u x n_h
Q_i	Thermal power generated by CHP units	n_m x n_u x n_h	n_m x n_u x n_h	n_m x n_u x n_h	n_m x n_u x n_h
δ_i	Inclusion/exclusion of CHP units	n_m x n_u x n_h	n_m x n_u x n_h	n_m x n_u x n_h	n_m x n_u x n_h
F_{gb}	Power content of input fuel of GBs	n_u x n_h	n_u x n_h	n_u x n_h	n_u x n_h
E_{sh}	Shared electric energy	-	-	n_h	n_h
n_{PV}	Number of PV panels	n_u	1	1	n_u
n_{TSC}	Number of TSC panels	n_u	n_u	n_u	n_u
C_{ees}	EES capacity	n_u	*1*	*1*	n_u
$P_{c,ees}$	EES charging electric power	n_u x n_h	n_u x n_h	n_u x n_h	n_u x n_h
$P_{d,ees}$	EES discharging electric power	n_u x n_h	n_u x n_h	n_u x n_h	n_u x n_h
$E_{ees}(h=1)$	Starting EES energy	n_u	*1*	*1*	n_u
V_{tes}	TES volume	n_u	n_u	n_u	n_u
$Q_{c,tes}$	TES charging thermal power	n_u x n_h	n_u x n_h	n_u x n_h	n_u x n_h
$Q_{d,tes}$	TES discharging thermal power	n_u x n_h	n_u x n_h	n_u x n_h	n_u x n_h
$V_{hot}(h=1)$	Starting TES hot water volume	n_u	n_u	n_u	n_u
Total number of decision variables		7794	7404	7500	7890

Differently, f_1 is defined for the CEC and REC configurations as follows:

$$f_1 = C_{ees} \cdot ef_{ees} + \sum_j V_{tes,j} \cdot ef_{tes} + \sum_{h=1}^{96} \Bigg[\left(P_{gw,h} - E_{sh,h}\right) ef_{eg} + P_{PV,h} \cdot ef_{PV} + \sum_j \Bigg(F_{gb,j,h} \cdot ef_{gb} + Q_{TSC,j,h} \cdot ef_{TSC} + \sum_i \delta_{i,j} \cdot F_{i,j,h} \cdot ef_i \Bigg) \Bigg], for \; j \in \{Res, Com1, Com2\} \; and \; i \in \{ice1, ice2, ice3, ice4\},$$

(18)

where E_{sh} is only defined for REC. In this case, the EES is shared among users and, therefore, the associated term C_{ees} is reported outside the summation in j.

f_2 is described by the following equation for the IP and HC configurations:

$$f_2 = \sum_j \Bigg\{ \Bigg[\sum_i \delta_{i,j} \left(C_{a,i} + c_{O\&M,fix,i} \right) P_{n,i} \Bigg] + n_{PV,j} \left(C_{a,PV} + c_{O\&M,fix,PV} \right) + n_{TSC,j} \left(C_{a,TSC} + c_{O\&M,fix,TSC} \right) + C_{ees,j} \left(C_{a,ees} + c_{O\&M,fix,ees} \right) + V_{tes,j} \left(C_{a,tes} + c_{O\&M,fix,tes} \right) \Bigg\} + \sum_{h=1}^{96} \Bigg\{ -E_{sh,h} \cdot p_{sh} + \sum_j \Bigg[c_{e,h} \cdot P_{gw,j,h} - p_{e,h} \cdot P_{gf,j,h} + F_{gb,j,h} \left(c_g + c_{O\&M,var,gb} \right) + \sum_i \delta_{i,j} \cdot F_{i,j,h} \left(c_{bg} + c_{O\&M,var,i} \right) \Bigg] \Bigg\}, for\ j \in \{Res, Com1, Com2\}\ and\ i \in \{ice1, ice2, ice3, ice4\}, \quad (19)$$

whereas $P_{gw,j}$, $P_{gf,j}$, n_{PV}, and C_{ess} are outside the summation in j for the CEC and REC. E_{sh} is only defined for the REC and HC.

2.2.3 Constraints

Constraints on the conversion and storage units are the same for all the configurations of prosumers and correspond to the equations presented in *Section 2.1.2*. On the contrary, the energy balances depend on the specific configuration of prosumers and are presented in *Section 2.1.4*. It is important to note that the constraint represented by *Eq. (3)*, i.e., the electric power generated by a CHP unit, is quadratic (two continuous variables, $\eta_{el,i}$ and F_i, multiply each other). Thus, it is only allowed by a MIQP algorithm. On the other hand, a MILP algorithm would require the electrical efficiency being constant to ensure the linearity of the constraint, imposing an excessively simplified representation of the real CHP unit.

Another relevant constraint is that the installed area of PV and TSC cannot exceed a maximum value that represents the available rooftop area (A_{roof}) of each building. A_{roof} is equal to 1200 m^2 for *Res*, 0 m^2 for *Com1* (no available rooftop area) and 400 m^2 for *Com2* [65].

2.3 Demand side management strategies

Two different demand side management (DSM) strategies are developed and applied to the electricity demand. The first approach is a price-based demand response (PBDR) program applied downstream of the design-operation optimization, whereas the second one is applied upstream of the design-operation optimization and aims at adapting the demand to the RES availability (i.e., to the solar radiation).

2.3.1 Price-Based Demand Response (PBDR) for a given EC design

The first approach is a PBDR program that considers hourly variations of the electricity selling price (p_e) and purchasing cost (c_e) due to the wholesale electricity market (see ***Figure 5***). The electricity demand is free to vary within well-defined bounds because of responding to the electricity price variations. The PBDR strategy is not directly integrated in the bi-objective design-operation

optimization discussed in *Section 2.2*, but is applied subsequently receiving the design optimization results as input. This strategy further economically optimizes the operation of the ECs by means of a single objective MILP algorithm, which has the hourly values of the electricity demand of each user as the only decision variables. At the end of the optimization procedure, the optimized demand values (D_{mod}) differ from those of the original demand (D_{el}).

It is assumed that loads can only be shifted within a day and not curtailed by the PBDR program applied here. Thus, the obtained overall daily demand of each user j must be equal to overall original demand:

$$\sum_{h=h_{start,s}}^{h_{end,s}} D_{mod,j,s,h} = \sum_{h=h_{start,s}}^{h_{end,s}} D_{el,j,s,h,}\, for\ j \in \{Res, Com1, Com2\}, and\ s \in \{winter, spring, summer, autumn\},$$

(20)

where h_{start} and h_{end} are the first and last hour of a specific typical day (s), respectively. Furthermore, there are some limitations on the load shifting because at any time a part of the load is necessary and cannot be avoided. For this reason, a constraint on the maximum relative hourly variation of the demand (ΔD_{max}) is imposed:

$$\left(1 - \Delta D_{max,j}\right) D_{el,j,h} \leq D_{mod,j,h} \leq \left(1 + \Delta D_{max,j}\right) D_{el,j,h}, for\ j \in \{Res, Com1, Com2\}\ and\ h \in [1,96],$$

(21)

where ΔD_{max} cannot be greater than 0.3 [38]. According to this upper bound, ΔD_{max} is assumed to be constant and equal to 0.3 for the residential users, to 0.2 and 0.1 for the first and second type of commercial users, respectively.

The only objective is the maximization of economic savings that PBDR can bring with respect to the case in which no DR strategy is applied subsequently of the bi-objective design-operation optimization.

2.3.2 Adapting demand to RES availability prior to EC design

To the knowledge of the authors, the second DSM approach proposed represents a novelty compared to the current literature. The profile of modified demand is not the outcome of an optimization algorithm but is analytically obtained to increase or decrease the required load when sunlight is available or not, respectively. Subsequently, the resulting demand profile of each configuration of prosumers is provided as input to the design-operation optimization described in *Section 2.2*.

The constraints described by *Eqs. (20)* and *(21)* are still valid. The only necessary data to be provided as input of this model are the original electricity demand (D_{el}) and the profile of solar irradiance (G_{β}). For each hour (h) of each typical day (s) the solar irradiance is normalised (G_{norm}) to its maximum value (G_{max}) of that day:

$$G_{norm,s,h} = \frac{G_{\beta,s,h}}{G_{max,s}}, for\ s \in \{winter, spring, summer, autumn\}.$$

(22)

An increase of the hourly demand (ΔD_{+}) proportional to the normalised irradiance is assigned to each user:

$$\Delta D_{+,j,s,h} = D_{el,j,s,h} \cdot \Delta D_{max,j} \cdot G_{norm,s,h}, for\ j \in \{Res, Com1, Com2\}\ and\ s \in \{winter, spring, summer, autumn\},$$

(23)

where $\Delta D_{max,j}$ has been already defined in *Section 2.3.1*. To maintain the daily demand constant, a curtailment must correspond to the total increase of demand associated with the integral of *Eq.(23)* over a typical day. To adapt the demand to the solar radiation availability, this curtailment must occur when no irradiance can be collected. The corresponding period of hours (τ_{nl}) is the entire day minus the time interval comprised between the appearance and disappearance of the sun beams. The relationship between τ_{nl} and the time interval in which solar radiation is available (τ_l) is the following:

$$24h = \tau_{nl,s} + \tau_{l,s}, for\ s \in \{winter, spring, summer, autumn\},$$

(24)

where s is in subscript because the hours of daylight depend on the characteristic seasonal day. The hourly demand curtailment (ΔD_{-}) is uniformly distributed in the hours of τ_{nl}:

$$\Delta D_{-,j,s,h} = \frac{1}{\tau_{nl,s}} \sum_{h=h_{start,s}}^{h_{end,s}} \Delta D_{+,j,s,h}\,, for\ j \in \{Res, Com1, Com2\}\ and\ s \in \{winter, spring, summer, autumn\},$$

(25)

where h_{start} and h_{end} are the first and last hour of a specific typical day (s), respectively. Since ΔD_{+} is zero in τ_{nl}, the summation of ΔD_{+} over the entire day corresponds to the one over τ_l. Thus, the modified demand (D_{mod}) is calculated by means of the following algorithm:

$$if\ h \in \tau_{l,s}\colon D_{mod,j,s,h} = D_{el,j,s,h} + \Delta D_{+,j,s,h};$$

$$else\ if\ h \in \tau_{nl,s}\colon D_{mod,j,s,h} = D_{el,j,s,h} - \Delta D_{-,j,s,h},$$

$$for\ j \in \{Res, Com1, Com2\}\ and\ s \in \{winter, spring, summer, autumn\}.$$

(26)

2.4 Key performance indicators

Four key performance indicators are analysed over the entire reference period to describe and compare the obtained results.

i) The total cost of energy ($TCOE$) is calculated as the total actualized cost (investment plus operation) of the energy supply, C_{tot}, divided by the total energy demand (electricity plus heat):

$$TCOE = \frac{C_{tot}}{D_{el,tot} + D_{th,tot}} \left[\frac{c€}{kWh}\right],$$

(27)

where the subscript *tot* refers to the summation over the entire reference period.

ii) The specific GHG emissions (EM_{CO2}) are calculated as the total GHG emissions, GHG_{tot}, divided by the total energy demand (electricity plus heat):

$$EM_{CO2} = \frac{GHG_{tot}}{D_{el,tot} + D_{th,tot}} \left[\frac{g_{CO2}}{kWh}\right].$$

(28)

iii) The self-consumption rate (SCR) is calculated as the amount of self-consumed electricity (virtually or physically) divided by the total electricity demand:

$$SCR = \frac{\sum_{h=1}^{96} min\{D_{el,h} + P_{ees,c,h}; P_{gen,h} + P_{ees,d,h}\}}{D_{el,tot}} 100\ [\%],$$

(29)

where P_{gen} is the sum of the electric power generated by all the available conversion units, $P_{ees,c}$ and $P_{ees,d}$ are the electric power flowing in to and out from the available EES, respectively.

iv) The grid usage (GU) is calculated as the sum of the electricity withdrawn from and injected to the grid (eventually net of the shared electric energy) divided by the total electricity demand:

$$GU = \frac{P_{gw,tot} + P_{gf,tot}}{D_{el,tot}} 100\ [\%], \qquad (30)$$

where P_{gw} and P_{gf} are the electric power withdrawn from and fed into the grid, respectively.

The indicators of the refence case (REF), i.e., simple consumers, are reported in ***Table 5***.

Table 5 *Resulting indicators for the reference case (REF).*

Performance indicator	Results of the reference case (REF)
TCOE	14.6 c€/kWh
EM_{CO2}	287.6 g/kWh
SCR	0 %
GU	100 %

3 Results

In this section the results obtained by the application of the proposed design-operation optimization and demand side management strategies to the different organizations of prosumers are presented.

3.1 Bi-objective design and operation optimization

3.1.1 Construction of the Pareto front

To obtain the Pareto front of a specific organization of prosumers as result of its design and operation optimization, the weights of the bi-objective function (w_1 and w_2) are iteratively varied 11 times, as reported in *Section 2.2*. By scaling f_2 and f_1 with the overall energy demand over the entire reference period, $TCOE$ and EM_{CO2} are obtained and placed on the x and y-axis of the Pareto front, respectively, without modifying the shape of the front itself. For instance, ***Figure 9*** reports the Pareto front of the CEC configuration. Note that some of the 11 resulting points can collapse into the same one because of the integer nature of the problem. Thus, ***Figure 9*** apparently shows only 7 points. As expected, EM_{CO2} decreases with increasing w_1, whereas TCE decreases with increasing w_2.

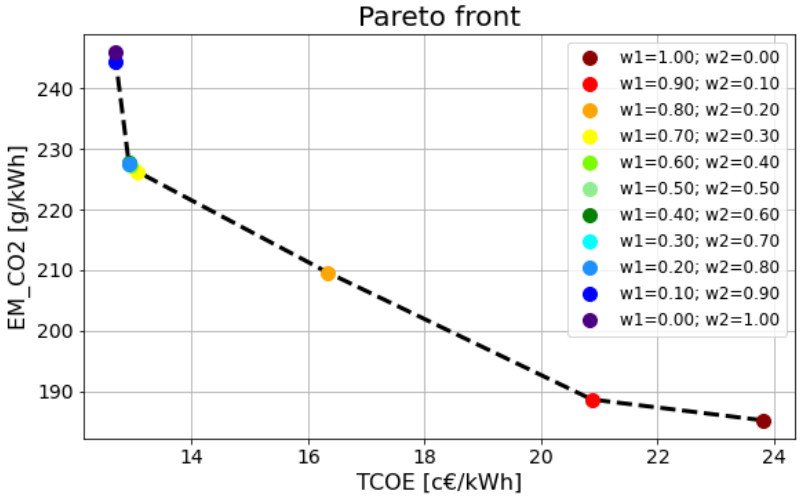

Figure 9 *Pareto front resulting from the design-operation optimization of the CEC configuration.*

3.1.2 Comparison of the Pareto fronts of the different organizations of prosumers

Figure 10 reports the comparison of the Pareto fronts obtained from the multi-objective design-operation optimization of each analysed organization of prosumers. The obtained GHG emissions are always lower than those of the reference case ($EM_{CO2,REF}$ = 287.5 g/kWh). Differently, the energy expenditure is lower than the reference case ($TCOE_{REF}$ = 14.6 c€/kWh) - i.e., the optimized configurations are cost effective - only when the economic objective becomes relevant ($w_2 \geq 0.3$). The advantages of the ECs over prosumers individually acting (IP) appear evident. When the cost is minimized (w_2 = 1), the $TCOE$ of ECs is from 13% (CEC) to 10% (REC) lower than the reference case, while EM_{CO2} reduces of about 14%. In the same conditions, the $TCOE$ of IP is only 6% lower than REF, and EM_{CO2} only reduces of 5%. The slight improvement in the economic results of the CEC compared to the HC and REC is mainly due to the valorisation of the shared electric energy (given by the incentive plus the electricity selling price) that is slightly lower than the savings (evaluated at the electricity purchasing cost) associated with the avoided electricity withdrawn from the grid. This favours the physical self-consumption (CEC) over the virtual one (REC and, partially, HC). When the GHG emissions are minimized (w_1 = 1), the EM_{CO2} of each EC configuration is 17% lower than IP and 36% lower than REF. However, in this case none of the configuration considered is cost-effective.

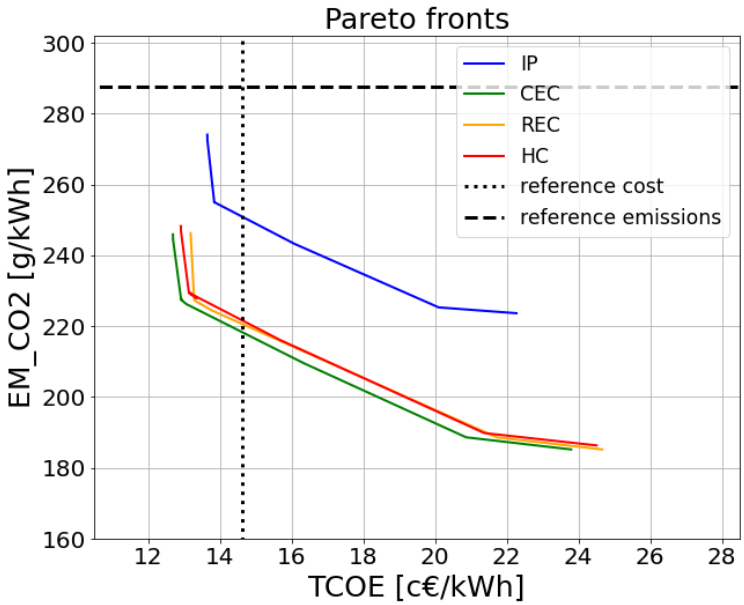

Figure 10 *Pareto fronts of the design-operation optimization of each configuration of prosumers.*

3.1.3 Optimal number, type and size of the involved conversion and storage units

Figure 11 shows the optimal size of the conversion and storage units for each configuration of prosumers and each weight of the two objectives. The installed PV area always grows with w_1 because of its low emission factor. Note that, since the commercial user *Com1* has no available rooftop area, PV is only installed by the two remaining users. Differently, the CHP units are chosen only when the economic objective prevails ($w_2 \geq 0.8$), because of their cost-effectiveness in providing both electric and thermal baseloads and their high direct GHG emissions. The exploitation of the CHP unit corresponds to a greater volume of installed TES, able to modulate the thermal power delivered by the ICE, and to a lower TSC area. It results that only one of the smallest ICEs (15 kW of nominal power) is chosen and it is operated by the residential prosumer having the highest overall thermal demand (see ***Figure 3***). The exploitation of CHP units is mainly limited by the low thermal demand of users in summer. Conversely to CHP, the EES is exploited only when the minimization

of emissions prevails ($w_1 \geq 0.8$). Indeed, in spite of the low emission factor, the investment cost of EES is too high to make it cost effective.

3.1.4 Optimal key performance indicators

Figure 12 shows the optimal performance indicators for each configuration of prosumers and each weight of the two objectives. Thanks to the shared electricity the self-consumption of ECs is always higher than the self-consumption of IP. This is clear especially for the intermediate weights ($0.3 \leq w_1 \leq 0.7$) where the SCR of ECs is almost double than the one of IP (about 40% and 20%, respectively). Conversely, for the same weights, the grid usage of IP is about 20% higher than the one of ECs, meaning that the aggregation of prosumers into ECs allows to enhance the local self-consumption of renewable energy thereby decreasing the stress on the electricity grid. Note that the higher SCR of ECs is due to the possibility of sharing, physically or virtually, the generated electricity. Thus, possible generation surpluses of a prosumer can be exploited to fulfil the demand of another user and the overall renewable generation can increase. Moreover, because of the relevant difference between the electricity purchasing cost and selling price, generating electricity for the self-consumption is much more cost-effective than selling electricity to the grid. Consequently, the economic result of ECs is better than IP, as shown by the Pareto fronts (***Figure 10***).

Since EM_{CO2} and $TCOE$ are the two competing objectives, they follow opposite trends. $TCOE$ increases slowly with w_1 when $w_1 \leq 0.8$, while abruptly increasing in correspondence of the EES adoption (as occurs to SCR). Conversely, in the same range, the emissions drop (as also GU). The lower GHG emissions of ECs compared to IP mainly depend on the larger area of PV installed that leads to a higher renewable generation of electricity.

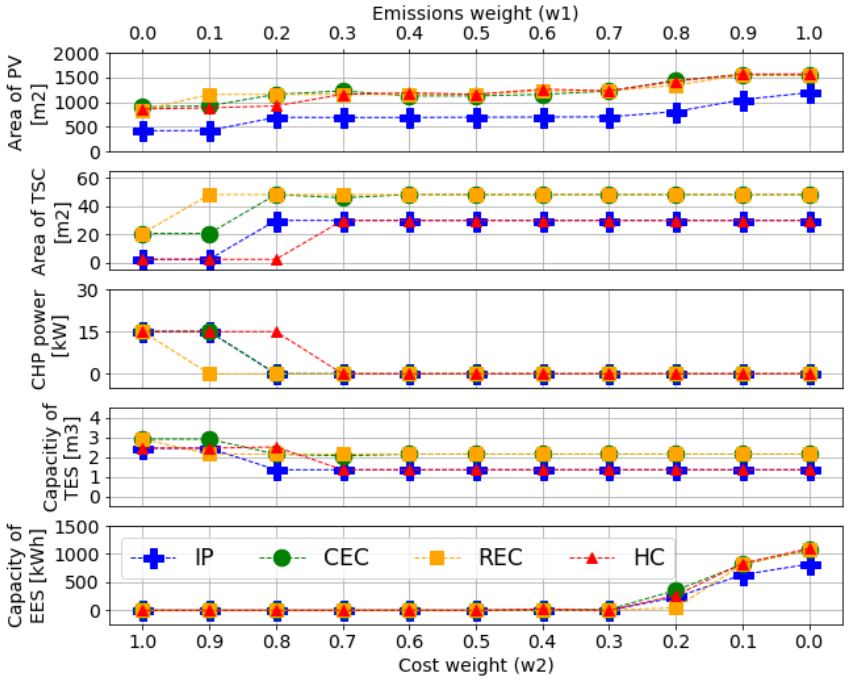

Figure 11 *Optimal size of the conversion and storage units as a function of the objective function weights for each organization of prosumers*

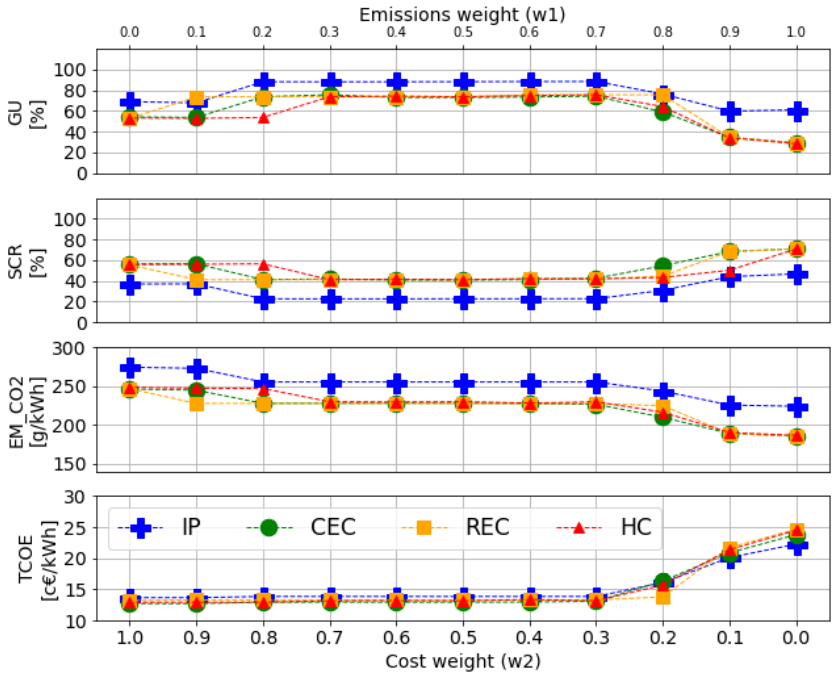

Figure 12 *Optimal values of the indicators as a function of the objective function weights for each organization of prosumers*

Table 6 reports the optimal values of the performance indicators and the sizes of the selected conversion and storage units in a specific trade-off point with w_1 = 0.4 and w_2 = 0.6. This trade-off point will be chosen hereinafter to compare the different configurations of prosumers analysed. Note that it allows obtaining a significant reduction in GHG emissions compared to the reference case, while maintaining the cost effectiveness of both EC and IP configurations. In fact, $TCOE$ and EM_{CO2} decrease of 5-12% and 11-21%, respectively, compared to REF and depending on the specific configuration.

Table 6 *Performance indicators and owned plants for a specific trade-off point of the design/operation optimization.*

Config.	w_1	w_2	*TCOE* [c€/kWh]	EM_{CO2} [g/kWh]	*SCR* [%]	*GU* [%]	Owned plants
REF	-	-	14.6	287.6	0	100	-
IP	0.4	0.6	13.8	255.0	22.5	88.2	689 m^2 of PV, 30 m^2 of TSC, 1.3 m^3 of TES
CEC	0.4	0.6	12.9	227.6	40.7	73.0	1125 m^2 of PV, 48 m^2 of TSC, 2.1 m^3 of TES
REC	0.4	0.6	13.3	227.4	41.1	72.8	1157 m^2 of PV, 48 m^2 of TSC, 2.1 m^3 of TES
HC	0.4	0.6	13.2	229.3	41.5	72.7	1189 m^2 of PV, 30 m^2 of TSC, 1.3 m^3 of TES

3.2 Demand side management

The two developed DSM strategies are:

- A single-objective optimization of the electrical demand by means of a PBDR program based on the hourly-variable electricity price and applied downstream of the design/operation optimization (DSM1);
- An analytical adaptation of the electricity demand to the solar radiation applied upstream of the design/operation optimization (DSM2).

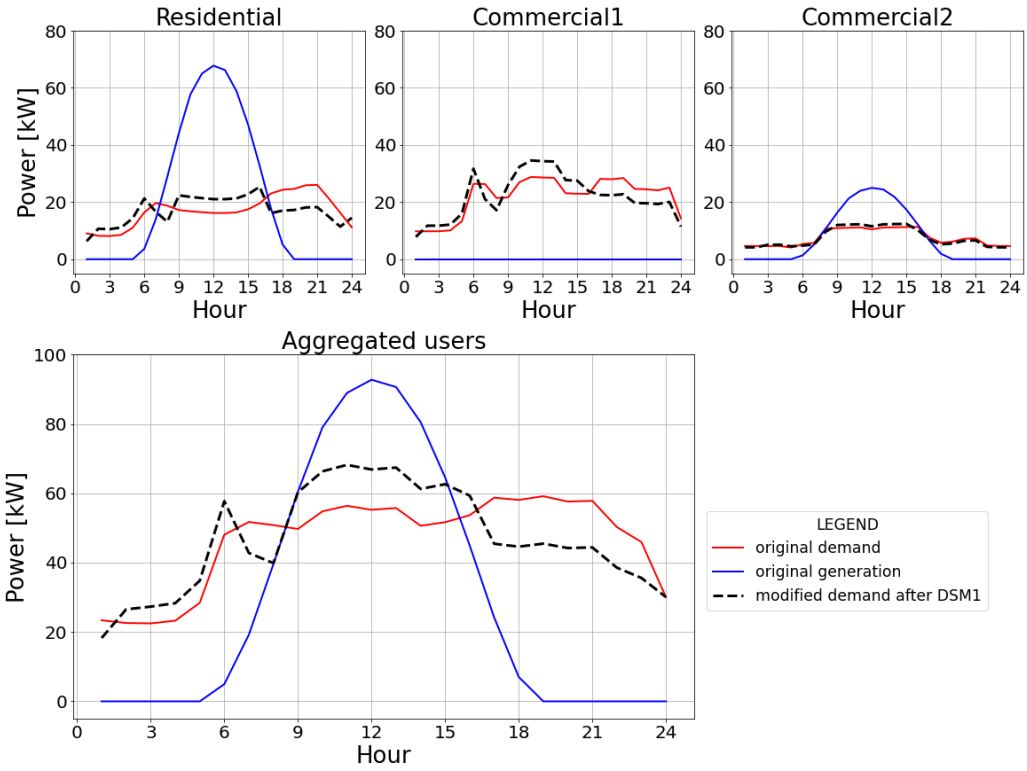

Figure 13 *Electricity demand and generation profiles after DSM1 (CEC configuration, typical spring day, $w_1 = 0.4$).*

The profiles of electricity demand and generation found by the application of DSM1 and DSM2 are reported in ***Figure 13*** and ***Figure 15*** , respectively. As an example, these profiles refer to the trade-off point with $w_1 = 0.4$ and $w_2 = 0.6$ of the typical spring day of the CEC. The spring day differs from the winter and summer ones mainly because of a higher and lower peak of PV generation, respectively. Differently, the daily profile of the electricity price is similar among the four seasons (apart from a slight decrease in its average value from winter to autumn, see ***Figure 14***), always having a peak in the morning and another one in the evening. It results that also the DSM trends are similar among all the seasonal typical days, and, therefore, only the spring day is described below as a reference.

Considering DSM1, the higher economic benefit of self-consuming, rather than selling electricity to the grid, entails on average an increase and decrease of the demand in correspondence of generation surpluses and defects, respectively. However, hour-by-hour variations of the demand may not strictly follow the average behaviour, showing, for example, instant increases outside the period of PV generation. The reason is that if an hourly value of the electricity purchasing cost is particularly low it can be convenient to shift part of the load toward that hour.

Differently, since DSM2 is applied upstream of the design phase, it also modifies the generation pattern. Due to the algorithm described in *Eq. (26)*, the demand growths when the solar radiation is available, especially around its peak (midday), and homogeneously decreases at night. The outcome is a larger installed surface of PV and, thus, an increased renewable generation of electricity compared to the case in which no DSM strategy is applied. Globally, the self-consumption rate increases, while the exchanges with the grid decrease.

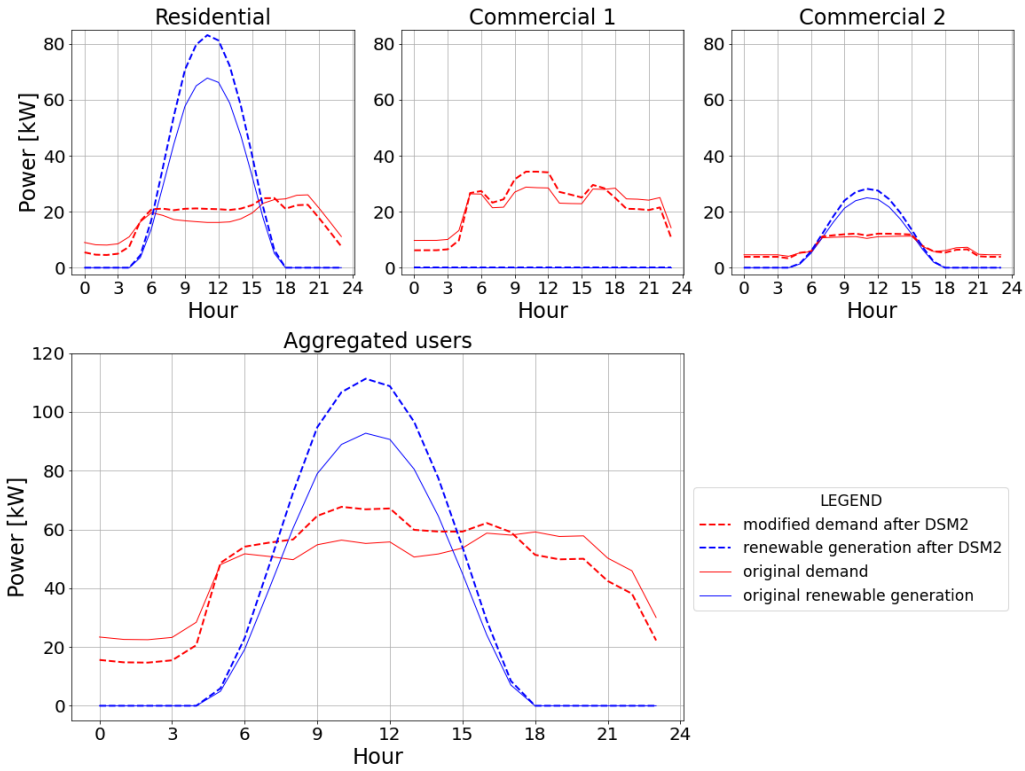

Figure 15 *Electricity demand and generation profiles after DSM2 (CEC configuration, typical spring day, w_1 = 0.4).*

Table 7 and ***Table 8*** report the values of the key performance indicators obtained by the application of DSM1 and DSM2, respectively, in the trade-off point with $w_1 = 0.4$ and $w_2 = 0.6$. The two tables show also next to each value (in brackets) the variation from the corresponding value in ***Table 6***, i.e., from the case of design-operation optimization without DSM. Both DSM strategies allow a very similar reduction of costs (-2% for IP and REC, -3% for CEC and HC) and emissions (-2% for IP, -4% for ECs) compared to the case of design-operation optimization without DSM (see ***Table 6***). Comparing the two strategies, DSM2 better promotes an increase in the self-consumption rate of both IP (+18%) and ECs (+16-18%), while DSM1 has a higher potential of reducing the exchanges with the grid (-7% for IP down to -15% for ECs) compared to the design-operation optimization without DSM.

Table 7 *Performance indicators in a trade-off point after DSM1 (in brackets the variation from* ***Table 6****).*

Config.	w_1	w_2	*TCOE* [c€/kWh]	EM_{CO2} [g/kWh]	*SCR* [%]	*GU* [%]
REF	-	-	14.6	287.6	0	100
IP	0.4	0.6	13.5 (-2.2%)	249.5 (-2.2%)	22.9 (+1.8%)	82.0 (-7.0%)
CEC	0.4	0.6	12.5 (-3.1%)	218.3 (-4.1%)	45.9 (+12.7%)	62.6 (-14.2%)
REC	0.4	0.6	13.0 (-2.3%)	218.0 (-4.1%)	46.4 (+12.9%)	62.0 (-14.8%)
HC	0.4	0.6	12.8 (-3.0%)	219.8 (-4.1%)	46.9 (+13.0%)	61.8 (-15.0%)

Table 8 *Performance indicators and owned PV in a trade-off point after DSM2 (in brackets the variation from* ***Table 6****).*

Config.	w_1	w_2	*TCOE* [c€/kWh]	EM_{CO2} [g/kWh]	*SCR* [%]	*GU* [%]	Owned PV [m^2]
REF	-	-	14.6	287.6	0	100	-
IP	0.4	0.6	13.7 (-0.7%)	249.6 (-2.1%)	26.6 (+18.2%)	85.5 (-3.1%)	803 (+16.5%)
CEC	0.4	0.6	12.6 (-2.3%)	217.8 (-4.3%)	48.2 (+18.4%)	68.7 (-5.9%)	1350 (+20.0%)
REC	0.4	0.6	13.0 (-2.3%)	217.7 (-4.3%)	48.4 (+17.8%)	68.4 (-6.0%)	1369 (+18.3%)
HC	0.4	0.6	12.8 (-3.0%)	219.8 (-4.1%)	48.4 (+16.6%)	68.4 (-5.9%)	1369 (+15.1%)

3.3 Critical remarks

Figure 16 compares the Pareto fronts after the design-operation optimization only (without DSM), after DSM1 and DSM2 strategies, and the reference values ($TCOE$ and EM_{CO2} of the reference case),

for each configuration of prosumers. The application of the DSM strategies modifies the Pareto fronts compared to the case without DSM.

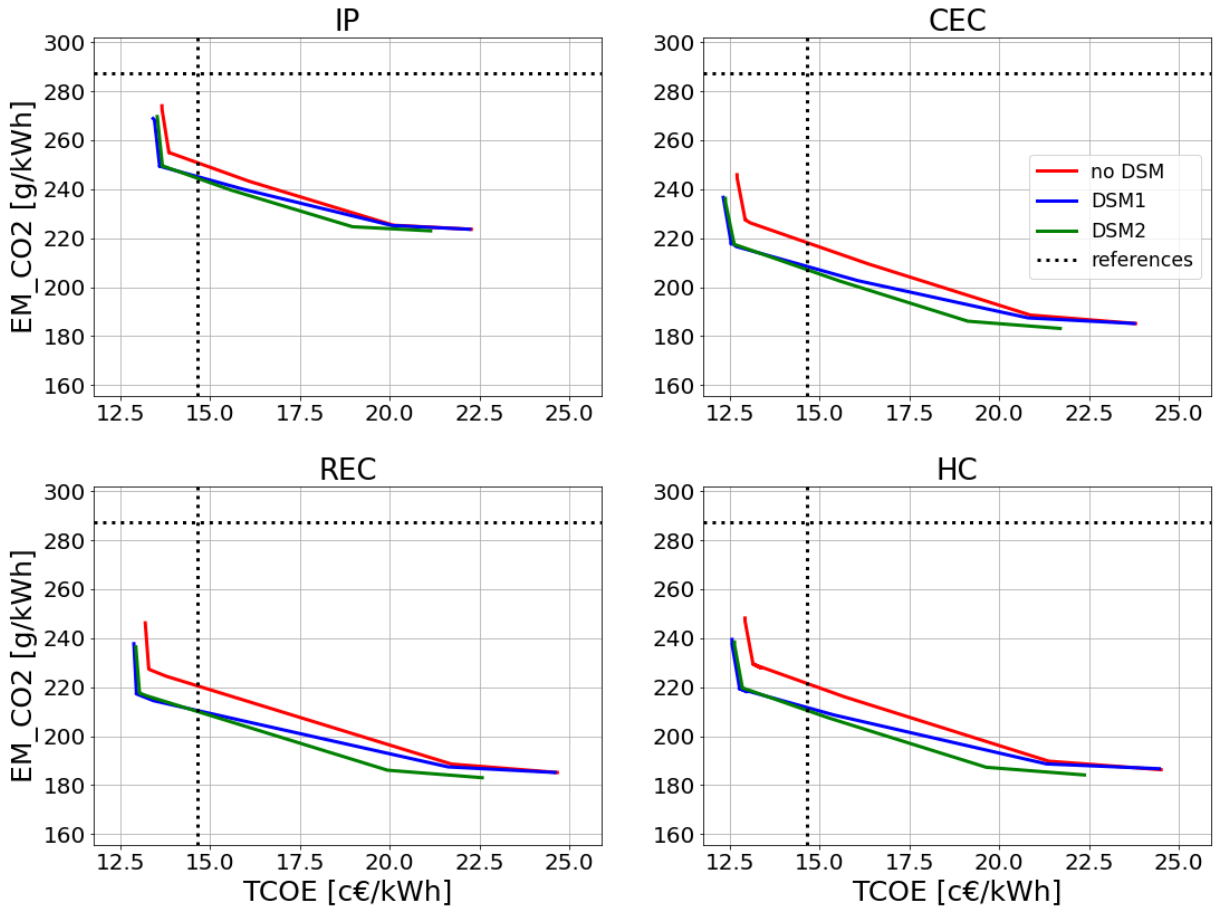

Figure 16 *Pareto fronts without DSM (design/operation optimization only), after DSM1 and DSM2, and reference values.*

Note that:

- The DSM1 strategy (i.e., the one applied downstream of the design phase) does not affect the generation patterns. When the economic objective prevails (high w_2, left side of the Pareto fronts), this strategy allows to reduce both costs and emissions compared to the design-operation optimization without DSM, because of the improvement in self-consumption and, consequently, the decrease in the electricity withdrawn from the grid (or the increase in the shared electric energy for REC and HC configurations). However, when the environmental objective prevails (high w_1, right side of the Pareto fronts), the self-consumption improvement is negligible or very limited because of the presence of the EES, which is charged by exploiting the generation surpluses, and discharged in correspondence of defects. Thus, also the reduction in cost and emissions becomes negligible (see the superimposition of red and blue lines in ***Figure 16***).
- Conversely, the DSM2 strategy (i.e., the one applied upstream of the design phase) affects the generation pattern. By adapting the electricity demand to the solar radiation, a larger area of PV can be deployed. This results in an improvement of the economic and environmental objectives throughout the entire Pareto front (the green line in ***Figure 16*** appears to be entirely shifted from the red one toward lower costs end emissions), while also improving the energetic performance indicators (SCR and GU).

Another important remark regards the distribution of the conversion units among the members of the community. The installation of CHP units results to be convenient only when the cost minimization prevails and only for the residential user, which has the highest thermal demand. Moreover, one of the two commercial users, having not any available rooftop area, cannot install either PV or TSC and, therefore, results to be a simple consumer rather than a prosumer (see, for instance, ***Figure 13*** or ***Figure 15***). However, this does not prevent that user to participate into an EC. In fact, the simple consumer contributes to improving the self-consumption of the entire community by partially consuming the generation surpluses due to the PV production of the two remaining prosumers. This benefits both the simple consumer, which can have access to cheaper electricity, and the other prosumers, which can generate higher incomes compared to directly selling generation surpluses to the grid. It is worth pointing out that the way the economic benefits could be allocated between the simple consumer and the prosumers is out of the scope of this paper. Conversely, when prosumers individually acting (IP) are considered, the simple consumer has not access to the above-mentioned surpluses of generation, thereby not apporting any benefits to either itself or the other prosumers. This is the main reason of the worse results achieved by the IP compared to ECs (see ***Figure 10***).

4 Conclusions

This paper investigates how local prosumers of renewable energy can aggregate into Energy Communities (ECs), with the aim of improving the economic performance of the ECs while contributing to address the issue of climate change.

The ECs are modelled in terms of mixed-integer-programming problems, mainly linear, with only a couple of constraints being quadratic to avoid excessive simplifications of the real systems (e.g., the characteristics of the internal combustion engines). Despite a certain degree of simplification associated with linearization is still present, adopting this method has been necessary to solve the proposed models within a reasonable computational time (about 30 minutes by using a computer with an Intel$^{(R)}$ Core$^{(TM)}$ i5-7200U CPU and 8 GB of RAM).

A multi-objective optimization searches for the best type, size (design) and operation of the energy conversion and storage units of the prosumers included into ECs in order to minimize both the overall cost (operation and investment) and greenhouse gas emissions (direct, due to fuel burning, and indirect, due to the life cycle). It results that combined heat and power (CHP) internal combustion engines are exploited only when the economic objective prevails and only by the user having the highest thermal demand. Conversely, PV results to be convenient both for minimizing costs (coupled to CHP) and for minimizing emissions (coupled to battery storage), while being distributed among all users having available rooftop area. ECs can contextually obtain up to 12% of economic savings and a reduction of greenhouse gas emissions of 21% compared to the reference case of passive users, which are almost double of the benefits achievable by the same prosumers individually acting. The better performances of ECs are mainly due to the wider installed area of PV, resulting in a higher free-of-charge renewable generation, and to the higher share of local self-consumption allowed by sharing electricity.

Subsequently, a new Demand Side Management (DSM) program is applied upstream of the multi-objective design-operation optimization to adapt the electricity demand of each prosumer to the available solar radiation. The electrical demand tends to increase in the middle hours of the day to allow prosumers self-consuming a greater share of the potential PV generation, while decreasing at night. Consequently, the installed area of PV and, therefore, the associated renewable generation increase of 15-20% compared to the design-operation optimization without DSM. This also ensures a better balancing between generation and demand profiles, thereby decreasing the usage of the electricity grid. The further improvements of the economic and environmental results achieved by ECs compared to the design-operation optimization without DSM (up to 3% and 4% of reduction in

costs and emissions, respectively) are in line with a price-based demand response program applied downstream of the EC design.

In summary, the following guidelines can be suggested:

- Generating electricity for the local self-consumption is more cost-effective than selling the generated electricity to the grid. Indeed, the almost double share of self-consumption compared to prosumers individually acting is the main reason of the better economic and environmental results achieved by ECs;
- A simple consumer not owning any conversion or storage unit can join and benefit the EC. In fact, the simple consumer allows improving the community level of self-consumption and, therefore, the economic savings, also by actively participating in DSM programs;
- Developing simpler configurations of ECs - as the proposed Hybrid Community, where users can exploit both individual and collective self-consumption - allows prosumers substantially improving the economic and environmental benefits with respect to what they would obtain if operate independently, while achieving results in line with more complex configurations as the Renewable or Citizen ECs.

As a last consideration, since the ECs are modelled as organizations of prosumers and no district heating network is considered, the thermal demand, differently from the electrical demand, must be individually fulfilled by each prosumer. Therefore, the exploitation of CHP units is limited by the low individual heating demands in summer, which make CHP units not cost effective and highly pollutant for the electricity generation only. Thus, further improvements of this work should consider the design of a possible district heating network that connects the community's members to verify whether sharing thermal energy can make convenient a wider exploitation of CHP (e.g., a centralized unit that fulfils the aggregated heating demand of the entire community).

Nomenclature

Abbreviations

CEC	Citizen Energy Community
CHP	Combined Heat and Power
DR	Demand Response
DSM	Demand Side Management
EC	Energy Community
EES	Electric Energy Storage
EU	European Union
GB	Gas Boiler
GHG	Greenhous Gas
HC	Hybrid Community
ICE	Internal Combustion Engine
IEMD	Internal Electricity Market Directive
IP	Individual Prosumers
MILP	Mixed Integer Linear Programming
MIQP	Mixed Integer Quadratic Programming
PBDR	Price Based Demand Response
PV	Photovoltaic
REC	Renewable Energy Community
RED II	Renewable Energy Directive (recast)
REF	Reference case (passive users)
TES	Thermal Energy Storage
TSC	Thermal Solar Collectors

Symbols

GU	Grid usage
EM_{CO2}	Specific CO_2-equivalent emissions
f_1	Economic objective function
f_2	Environmental objective function
$TCOE$	Total cost of energy
SCR	Self-consumption rate
w_1	Weight of f_1
w_2	Weight of f_2

Acknowledgments

This research did not receive any specific grant from funding agencies in the public, commercial, or not-for-profit sectors.

References

[1] UNFCC. *The Paris Agreement*. Available: https://unfccc.int/process-and-meetings/the-paris-agreement/the-paris-agreement

[2] European Commission. *Clean Energy for All Europeans package*. Available: https://ec.europa.eu/energy/topics/energy-strategy/clean-energy-all-europeans_en
[3] European Commission. *'Fit for 55': delivering the EU's 2030 Climate Target on the way to climate neutrality*. Available: https://eur-lex.europa.eu/legal-content/EN/TXT/PDF/?uri=CELEX:52021DC0550&from=HR
[4] ClimateWatch. *Historical GHG emissions*. Available: https://www.climatewatchdata.org/ghg-emissions?end_year=2018&start_year=1990
[5] E. Caramizaru and A. Uihlein, "Energy communities: an overview of energy and social innovation," Publications Office of the European Union, Luxembourg2020. doi:10.2760/180576.
[6] J. Lowitzsch, C. E. Hoicka, and F. J. v. Tulder, "Renewable energy communities under the 2019 European Clean Energy Package – Governance model for the energy clusters of the future?," *Renewable and Sustainable Energy Reviews,* vol. 122, p. 109489, 2020. https://doi.org/10.1016/j.rser.2019.109489.
[7] EU, *Directive (EU) 2018/2001 of the European Parliament and of the Council*, 2018. https://eur-lex.europa.eu/legal-content/EN/TXT/PDF/?uri=CELEX:32018L2001&from=EN
[8] EU, *Directive (EU) 2019/944 of the European Parliament and of the Council*, 2019. https://eur-lex.europa.eu/legal-content/EN/TXT/PDF/?uri=CELEX:32019L0944&from=EN
[9] ARERA, *Regolazione delle partite economiche relative all'energia elettrica condivisa da un gruppo di autoconsumatori di energia rinnovabile che agiscono collettivamente in edifici o condomini oppure condivisa in una comunità di energia rinnovabile*, 2020. https://www.arera.it/allegati/docs/20/318-20alla.pdf
[10] GSE, *Gruppi di autoconsumatori e comunità di energia rinnovabile*, 2020. https://www.gse.it/servizi-per-te/autoconsumo/gruppi-di-autoconsumatori-e-comunita-di-energia-rinnovabile
[11] ARERA. (2020). *Bilancio Energetico Nazionale*. Available: https://www.arera.it/it/dati/bilancio_en.htm
[12] infodata, "Pmi, quanto conta in Italia il 92% delle aziende attive sul territorio?," *Il Sole 24 Ore,* 2019. https://www.infodata.ilsole24ore.com/2019/07/10/40229/
[13] V. Gjorgievski, S. Cundeva, and G. Georghiou, "Social arrangements, technical designs and impacts of energy communities: A review," *Renewable Energy,* vol. 169, pp. 1138-1156, 2021. doi:10.1016/j.renene.2021.01.078.
[14] S. Rech, "Smart Energy Systems: Guidelines for Modelling and Optimizing a Fleet of Units of Different Configurations," *Energies,* vol. 12, p. 1320, 2019. doi:10.3390/en12071320. https://www.mdpi.com/1996-1073/12/7/1320
[15] A. L. Berka and E. Creamer, "Taking stock of the local impacts of community owned renewable energy: A review and research agenda," *Renewable and Sustainable Energy Reviews,* vol. 82, pp. 3400-3419, 2018. https://doi.org/10.1016/j.rser.2017.10.050.
[16] F. Hanke and J. Lowitzsch, "Empowering Vulnerable Consumers to Join Renewable Energy Communities—Towards an Inclusive Design of the Clean Energy Package," *Energies,* vol. 13, p. 1615, 2020. doi:10.3390/en13071615. https://www.mdpi.com/1996-1073/13/7/1615
[17] E. Barbour, D. Parra, Z. Awwad, and M. C. González, "Community energy storage: A smart choice for the smart grid?," *Applied Energy,* vol. 212, pp. 489-497, 2018. https://doi.org/10.1016/j.apenergy.2017.12.056.
[18] F. Ceglia, E. Marrasso, C. Roselli, and M. Sasso, "Small Renewable Energy Community: The Role of Energy and Environmental Indicators for Power Grid," *Sustainability,* vol. 13, p. 2137, 2021. doi:10.3390/su13042137. https://www.mdpi.com/2071-1050/13/4/2137
[19] M. Cossutta, S. Pholboon, J. McKechnie, and M. Sumner, "Techno-economic and environmental analysis of community energy management for peak shaving," *Energy Conversion and Management,* vol. 251, p. 114900, 2022. https://doi.org/10.1016/j.enconman.2021.114900.
[20] C. Hachem-Vermette, F. Guarino, V. La Rocca, and M. Cellura, "Towards achieving net-zero energy communities: Investigation of design strategies and seasonal solar collection and storage net-zero," *Solar Energy,* vol. 192, pp. 169-185, 2019. https://doi.org/10.1016/j.solener.2018.07.024.
[21] G. Chehade and I. Dincer, "Development and analysis of a polygenerational smart energy hub for sustainable communities," *Energy Conversion and Management,* vol. 226, p. 113475, 2020. https://doi.org/10.1016/j.enconman.2020.113475.
[22] Y. He, Y. Zhou, J. Yuan, Z. Liu, Z. Wang, and G. Zhang, "Transformation towards a carbon-neutral residential community with hydrogen economy and advanced energy management strategies," *Energy Conversion and Management,* vol. 249, p. 114834, 2021. https://doi.org/10.1016/j.enconman.2021.114834.
[23] B. Vand, R. Ruusu, A. Hasan, and B. Manrique Delgado, "Optimal management of energy sharing in a community of buildings using a model predictive control," *Energy Conversion and Management,* vol. 239, p. 114178, 2021. https://doi.org/10.1016/j.enconman.2021.114178.
[24] S. Bracco, F. Delfino, G. Ferro, L. Pagnini, M. Robba, and M. Rossi, "Energy planning of sustainable districts: Towards the exploitation of small size intermittent renewables in urban areas," *Applied Energy,* vol. 228, pp. 2288-2297, 2018. doi:10.1016/j.apenergy.2018.07.074.
[25] S. Ruiz, J. Patiño, A. Marquez-Ruiz, J. Espinosa, E. Duque, and P. Ortiz, "Optimal Design of a Diesel-PV-Wind-Battery-Hydro Pumped POWER system with the Integration of ELECTRIC vehicles in a Colombian

Community," *Energies,* vol. 12, p. 4542, 2019. doi:10.3390/en12234542. https://www.mdpi.com/1996-1073/12/23/4542

[26] L. Novoa, R. Flores, and J. Brouwer, "Optimal renewable generation and battery storage sizing and siting considering local transformer limits," *Applied Energy,* vol. 256, 2019. doi:10.1016/j.apenergy.2019.113926.

[27] B. Yan, M. Di Somma, G. Graditi, and P. B. Luh, "Markovian-based stochastic operation optimization of multiple distributed energy systems with renewables in a local energy community," *Electric Power Systems Research,* vol. 186, p. 106364, 2020. https://doi.org/10.1016/j.epsr.2020.106364.

[28] Z. Liu, G. Fan, D. Sun, D. Wu, J. Guo, S. Zhang, *et al.*, "A novel distributed energy system combining hybrid energy storage and a multi-objective optimization method for nearly zero-energy communities and buildings," *Energy,* vol. 239, p. 122577, 2022. https://doi.org/10.1016/j.energy.2021.122577.

[29] H. ur Rehman, F. Reda, S. Paiho, and A. Hasan, "Towards positive energy communities at high latitudes," *Energy Conversion and Management,* vol. 196, pp. 175-195, 2019. https://doi.org/10.1016/j.enconman.2019.06.005.

[30] J. Guo, P. Zhang, D. Wu, Z. Liu, X. Liu, S. Zhang, *et al.*, "Multi-objective optimization design and multi-attribute decision-making method of a distributed energy system based on nearly zero-energy community load forecasting," *Energy,* vol. 239, p. 122124, 2022. https://doi.org/10.1016/j.energy.2021.122124.

[31] S.-H. Park, Y.-S. Jang, and E.-J. Kim, "Multi-objective optimization for sizing multi-source renewable energy systems in the community center of a residential apartment complex," *Energy Conversion and Management,* vol. 244, p. 114446, 2021. https://doi.org/10.1016/j.enconman.2021.114446.

[32] A. Fleischhacker, G. Lettner, D. Schwabeneder, and H. Auer, "Portfolio optimization of energy communities to meet reductions in costs and emissions," *Energy,* vol. 173, pp. 1092-1105, 2019. https://doi.org/10.1016/j.energy.2019.02.104.

[33] Z. Liu, J. Guo, D. Wu, G. Fan, S. Zhang, X. Yang, *et al.*, "Two-phase collaborative optimization and operation strategy for a new distributed energy system that combines multi-energy storage for a nearly zero energy community," *Energy Conversion and Management,* vol. 230, p. 113800, 2021. https://doi.org/10.1016/j.enconman.2020.113800.

[34] M. Castillo-Cagigal, A. Gutiérrez, F. Monasterio-Huelin, E. Caamaño-Martín, D. Masa, and J. Jiménez-Leube, "A semi-distributed electric demand-side management system with PV generation for self-consumption enhancement," *Energy Conversion and Management,* vol. 52, pp. 2659-2666, 2011. https://doi.org/10.1016/j.enconman.2011.01.017.

[35] L. Gelazanskas and K. A. A. Gamage, "Demand side management in smart grid: A review and proposals for future direction," *Sustainable Cities and Society,* vol. 11, pp. 22-30, 2014. https://doi.org/10.1016/j.scs.2013.11.001.

[36] V. Stavrakas and A. Flamos, "A modular high-resolution demand-side management model to quantify benefits of demand-flexibility in the residential sector," *Energy Conversion and Management,* vol. 205, p. 112339, 2020. https://doi.org/10.1016/j.enconman.2019.112339.

[37] U.S. Department of Energy, "Benefits of Demand Response in Electricity Markets and Reccomandations for Achieving them - A Report to the United States Congress Pursuant to Section 1252 of the Energy Policy Act of 2005," 2006.

[38] P. Li, Z. Wang, N. Wang, W. Yang, M. Li, X. Zhou, *et al.*, "Stochastic robust optimal operation of community integrated energy system based on integrated demand response," *International Journal of Electrical Power & Energy Systems,* vol. 128, p. 106735, 2021. https://doi.org/10.1016/j.ijepes.2020.106735.

[39] L. Li and S. Yu, "Optimal management of multi-stakeholder distributed energy systems in low-carbon communities considering demand response resources and carbon tax," *Sustainable Cities and Society,* vol. 61, p. 102230, 2020. https://doi.org/10.1016/j.scs.2020.102230.

[40] R. Barreto, P. Faria, C. Silva, and Z. Vale, "Clustering Direct Load Control Appliances in the Context of Demand Response Programs in Energy Communities," 2021. doi:10.1016/j.ifacol.2020.12.1827.

[41] S. Zhou, F. Zou, Z. Wu, W. Gu, Q. Hong, and C. Booth, "A smart community energy management scheme considering user dominated demand side response and P2P trading," *International Journal of Electrical Power & Energy Systems,* vol. 114, p. 105378, 2020. https://doi.org/10.1016/j.ijepes.2019.105378.

[42] *Gurobi Optimization*. Available: https://www.gurobi.com/

[43] L. Urbanucci, "Limits and potentials of Mixed Integer Linear Programming methods for optimization of polygeneration energy systems," *Energy Procedia,* vol. 148, pp. 1199-1205, 2018. https://doi.org/10.1016/j.egypro.2018.08.021.

[44] U.S. Department of Energy. *Open EI*. Available: https://openei.org/datasets/files/961/pub/

[45] European Commission. *PVGIS*. Available: https://re.jrc.ec.europa.eu/pvg_tools/it/#MR

[46] GME. *Dati storici MGP*. Available: https://www.mercatoelettrico.org/it/download/DatiStorici.aspx

[47] ARERA. (2022). *Dati statistici (Statistical data)*. Available: https://www.arera.it/it/dati/elenco_dati.htm

[48] S. Rech and A. Lazzaretto, "Smart rules and thermal, electric and hydro storages for the optimum operation of a renewable energy system," *Energy,* vol. 147, pp. 742-756, 2018. https://doi.org/10.1016/j.energy.2018.01.079.

[49] C.-Y. Park, S.-H. Hong, S.-C. Lim, B.-S. Song, S.-W. Park, J.-H. Huh*, et al.*, "Inverter Efficiency Analysis Model Based on Solar Power Estimation Using Solar Radiation," *Processes,* vol. 8, p. 1225, 2020. doi:10.3390/pr8101225. https://www.mdpi.com/2227-9717/8/10/1225

[50] M. Z. Jacobson and V. Jadhav, "World estimates of PV optimal tilt angles and ratios of sunlight incident upon tilted and tracked PV panels relative to horizontal panels," *Solar Energy,* vol. 169, pp. 55-66, 2018. https://doi.org/10.1016/j.solener.2018.04.030.

[51] B. Y. H. Liu and R. C. Jordan, "The interrelationship and characteristic distribution of direct, diffuse and total solar radiation," *Solar Energy,* vol. 4, pp. 1-19, 1960. https://doi.org/10.1016/0038-092X(60)90062-1.

[52] A. Jakhrani, A.-K. Othman, A. Rigit, S. Samo, and S. Kamboh, "Estimation of Incident Solar Radiation on Tilted Surface by Different Empirical Methods," *International Journal of Scientific and Research Publications,* vol. 2, pp. 1-6, 2012.

[53] K. Darrow, J. W. R. Tidball, and A. Hampson, "Catalog of CHP Technologies," U. S. E. P. Agency, Ed., ed, 2017.

[54] H. Abdi, B. Mohammadi-ivatloo, S. Javadi, A. Khodaei, and E. Dehnavi, "Energy Storage Systems," *Distributed Generation Systems: Design, Operation and Grid Integration,* pp. 333-368, 2017. doi:10.1016/B978-0-12-804208-3.00007-8.

[55] S. Campanari, "La cogenerazione: tecnologie, mercato, incentivi," Convegno Polygen: Cogenerazione Diffusa e Trigenerazione, Fiera di Milano2013.

[56] I. Sarbu and C. Sebarchievici, "A Comprehensive Review of Thermal Energy Storage," *Sustainability,* vol. 10, p. 191, 2018. doi:10.3390/su10010191. https://www.mdpi.com/2071-1050/10/1/191

[57] U.S. Department of Energy. *NREL Transforming Energy*. Available: www.nrel.gov/analysis/tech-cost-om-dg.html

[58] B. Fina, A. Fleischhacker, H. Auer, and G. Lettner, "Economic Assessment and Business Models of Rooftop Photovoltaic Systems in Multiapartment Buildings: Case Studies for Austria and Germany," *Journal of Renewable Energy,* vol. 2018, p. 9759680, 2018/02/20 2018. https://doi.org/10.1155/2018/9759680.

[59] Q. Dai, J. C. Kelly, L. Gaines, and M. Wang, "Life Cycle Analysis of Lithium-Ion Batteries for Automotive Applications," *Batteries,* vol. 5, p. 48, 2019. doi:10.3390/batteries5020048. https://www.mdpi.com/2313-0105/5/2/48

[60] M. Milousi, M. Souliotis, G. Arampatzis, and S. Papaefthimiou, "Evaluating the Environmental Performance of Solar Energy Systems Through a Combined Life Cycle Assessment and Cost Analysis," *Sustainability,* vol. 11, p. 2539, 2019. doi:10.3390/su11092539. https://www.mdpi.com/2071-1050/11/9/2539

[61] NREL, G. Heath, C. Turchi, J. Burkhardt, C. Kutscher, and T. Decker, "Conference Paper Life Cycle Assessment of Thermal Energy Storage: Two-Tank Indirect and Thermocline," vol. 2, 2009. doi:10.1115/ES2009-90402.

[62] R. Turconi, A. Boldrin, and T. Astrup, "Life cycle assessment (LCA) of electricity generation technologies: Overview, comparability and limitations," *Renewable and Sustainable Energy Reviews,* vol. 28, pp. 555-565, 2013. https://doi.org/10.1016/j.rser.2013.08.013.

[63] A. Fichera, E. Marrasso, M. Sasso, and R. Volpe, "Energy, Environmental and Economic Performance of an Urban Community Hybrid Distributed Energy System," *Energies,* vol. 13, p. 2545, 2020. doi:10.3390/en13102545. https://www.mdpi.com/1996-1073/13/10/2545

[64] A. Lazzaretto and A. Toffolo, "Energy, economy and environment as objectives in multi-criterion optimization of thermal systems design," *Energy,* vol. 29, pp. 1139-1157, 2004. doi:10.1016/j.energy.2004.02.022.

[65] J. Melius, R. M. Margolis, and S. Ong, "Estimating Rooftop Suitability for PV: A Review of Methods, Patents, and Validation Techniques," 2013. https://doi.org/10.2172/1117057.